Large-scale study of the interactions between proteins involved in type IV pilus biology in *Neisseria meningitidis*: characterization of a sub-complex involved in pilus assembly

Michaella Georgiadou [1], Marta Castagnini [1], Gouzel Karimova [2], Daniel Ladant [2] and Vladimir Pelicic [1,*]

[1] Section of Microbiology, Imperial College London, London, UK

[2] Unité de Biochimie des Interactions Macromoléculaires, CNRS URA 2185, Institut Pasteur, Paris, France

*To whom correspondence should be addressed. E-mail: v.pelicic@imperial.ac.uk

Abstract

The functionally versatile type IV pili (Tfp) are one of the most widespread virulence factors in bacteria. However, despite generating much research interest for decades, the molecular mechanisms underpinning the various aspects of Tfp biology remain poorly understood, mainly because of the complexity of the system. In the human pathogen *Neisseria meningitidis* for example, 23 proteins are dedicated to Tfp biology, 15 of which are essential for pilus biogenesis. One of the important gaps in our knowledge concerns the topology of this multi-protein machinery. Here we have used a bacterial two-hybrid system to identify and quantify the interactions between 11 Pil proteins from *N. meningitidis*. We identified 20 different binary interactions, many of which are novel. This represents the most complex interaction network between Pil proteins reported to date and indicates, among other things, that PilE, PilM, PilN and PilO, which are involved in pilus assembly, indeed interact. We focused our efforts on this subset of proteins and used a battery of assays to determine the membrane topology of PilN and PilO, map the interaction domains between PilE, PilM, PilN and PilO, and show that a widely conserved N-terminal motif in PilN is essential for both PilM-PilN interactions and pilus assembly. Finally, we show that PilP (another protein involved in pilus assembly) forms a complex with PilM, PilN and PilO. Taken together, these findings have numerous implications for understanding Tfp biology and provide a useful blueprint for future studies.

Introduction

The hair-like filaments known as pili (or fimbriae) that extend from the surface of numerous species are arguably bacterial favourite colonization factor (Sauer *et al.*, 2000). In pathogenic species, pili mediate bacterial adhesion to host cells and the extracellular matrix, and play a central role in the establishment of infection. Therefore, pili continue to be intensively studied as they represent primary targets for the development of new therapies against bacterial pathogens that impose a heavy burden on human health and economy by infecting mankind, livestock and crops. Among the multiple types of pili that have been identified, none are as widespread as type IV pili, Tfp (Pelicic, 2008). Tfp might be present in 150 different species spanning most bacterial phyla and are the only pili present in both Gram-negative and Gram-positive bacteria. This is likely a consequence of their functional versatility since in addition to their role in promoting attachment to a variety of biotic and abiotic surfaces, Tfp often mediate bacterial aggregation, uptake of DNA during transformation and twitching motility (Mattick, 2002). This versatility results from a remarkable capacity to retract and thereby generate mechanical force (Merz *et al.*, 2000; Maier *et al.*, 2002).

Tfp are morphologically similar in different species, *i.e*. they are thin, long and flexible filaments that often interact laterally to form bundles, and they share a number of sequence and structural characteristics (Craig *et al.*, 2004). They are predominantly polymers of one protein named pilin (PilE in *N. meningitidis'* nomenclature used throughout this manuscript). Pilins, which are synthesized as preproteins, have a conserved N-terminus encompassing a leader peptide that is cleaved by a prepilin peptidase, PilD (Strom *et al.*, 1993). Although the length of the leader peptide and mature protein define two distinct pilus subtypes named type IVa (Tfpa) and type IVb (Tfpb), the first one of which is by far the most widespread (Pelicic, 2008), all pilins have similar "lollipop" structures with a globular head and a stick formed by an extended N-terminal α-helix (Craig and Li, 2008). This hydrophobic α-helix

represents the major assembly interface between subunits and is packed within the interior of the filament in a helical fashion (Craig and Li, 2008).

Intensive efforts for more than two decades, mainly in human pathogens such as enteropathogenic *Escherichia coli* (EPEC), *Neisseria gonorrhoeae*, *N. meningitidis*, *Pseudomonas aeruginosa* and *Vibrio cholerae*, have resulted in the identification of probably all the proteins dedicated to Tfp biology (Pelicic, 2008). However, the molecular mechanisms underlying Tfp biogenesis and most Tfp-mediated functions are still to be elucidated. This is mainly due to the complexity of the system, with between 10 and 18 proteins necessary for Tfp biogenesis in *V. cholerae* and *P. aeruginosa* respectively, and several other proteins that modulate Tfp-linked functions. For example, a systematic analysis in *N. meningitidis* has shown that 15 proteins are essential for Tfp biogenesis (PilC1/PilC2, PilD, PilE, PilF, PilG, PilH, PilI, PilJ, PilK, PilM, PilN, PilO, PilP, PilQ and PilW), while seven (ComP, PilT, PilT2, PilU, PilV, PilX and PilZ) are dispensable for piliation but fine-tune Tfp-linked functions (Carbonnelle *et al.*, 2005; Brown *et al.*, 2010). The 15 proteins essential for Tfp biogenesis are conserved in sequence and genomic organization in bacteria expressing Tfpa, even in phylogenetically distant species, which suggests that a common mechanism is involved (Pelicic, 2008). Although mutants in the corresponding *pil* genes are invariably non-piliated, studies in *Neisseria* species have demonstrated that these proteins act at different stages of pilus biogenesis (Wolfgang *et al.*, 1998; Wolfgang *et al.*, 2000; Carbonnelle *et al.*, 2005). In *N. meningitidis*, piliation could be restored in the absence of eight of the above 15 proteins when pilus retraction is abolished by a concurrent mutation in *pilT* that encodes the traffic ATPase powering disassembly of pilins from Tfp (Carbonnelle *et al.*, 2006). Therefore, eight Pil proteins are dispensable for pilus assembly *per se*, indicating that pilus assembly is simpler than expected and may require "only" PilD, PilE, PilF, PilM, PilN, PilO and PilP.

The exact function of an overwhelming majority of the Pil proteins is still to be determined. The elucidation of the structure of some of them, *e.g*. PilE (Parge *et al.*, 1995),

92 has improved our understanding of several aspects of Tfp biology. However, it is widely
93 accepted that most of these proteins exert their action within a large multi-protein complex.
94 Therefore, further advances in our understanding of Tfp biology necessitate the
95 characterization of this machinery by identifying the underlying protein-protein interactions.
96 Systematic studies to unravel these interactions have been conducted in EPEC that express
97 Tfpb known as bundle-forming pili (Bfp). This has been done (i) by determining stability of
98 every Bfp protein by immunoblotting in mutants habouring in-frame deletions in each *bfp*
99 gene (the rationale being that the absence of one Bfp protein might result in
100 instability/degradation of interacting partners) (Ramer *et al.*, 2002), and (ii) by chemical
101 cross-linking and affinity purification of a large protein complex and identification of all the
102 interacting partners by immunoblotting (Hwang *et al.*, 2003). Unfortunately, due to the
103 important differences between the two Tfp subtypes (Pelicic, 2008), these results cannot be
104 easily extrapolated to Tfpa-expressing bacteria where less is known about Pil-Pil interactions
105 and the topography of the resulting machinery. Indeed, no similar systematic studies have
106 been conducted in bacteria expressing Tfpa where only a handful of Pil-Pil interactions have
107 been identified by a variety of approaches including (i) decreased stability of one protein in
108 the absence of others, *i.e*. PilW-PilQ and PilM-PilN-PilO-PilP (Carbonnelle *et al.*, 2005;
109 Ayers *et al.*, 2009), (ii) yeast two-hybrid, *i.e*. PilZ-PilF (Guzzo *et al.*, 2009), (iii) co-purification
110 of recombinant proteins, *i.e*. PilN-PilO and PilN-PilO-PilP (Sampaleanu *et al.*, 2009;
111 Tammam *et al.*, 2011), and (iv) co-crystallization, *i.e*. PilM-PilN (Karuppiah and Derrick,
112 2011). Interestingly, some of these studies have confirmed the important similarities with the
113 type II secretion machinery, a system that mediates the passage of folded proteins through
114 the outer membrane in Gram negative bacteria, which is evolutionarily related to Tfp
115 biogenesis and is thought to function by a similar mechanism (Ayers *et al.*, 2010).
116 Extending the frontiers of knowledge in Tfpa biology necessitates a better
117 understanding of the composition and organization of this multi-protein machinery.

Therefore, in the present study, we have adressed this issue by first identifying multiple interactions between 11 *N. meningitidis* Pil proteins using a bacterial two-hybrid system and then by performing a detailed functional analysis of a sub-complex involved in pilus assembly using a combination of approaches.

Results

Identification and quantification of protein-protein interactions between 11 N. meningitidis Pil proteins

Although two-hybrid methodology can identify protein-protein interactions on a large-scale and help charting protein networks involved in virtually any biological process (Uetz and Hughes, 2000), it has not been used systematically in Tfp biology. We opted for the bacterial adenylate cyclase two-hybrid (BACTH) system in which studied proteins are co-expressed in a *E. coli cya* mutant as fusions with one of two fragments (T18 and T25) from the catalytic domain of *Bordetella pertussis* adenylate cyclase (Karimova *et al.*, 1998). Interaction of two hybrid proteins results in a functional complementation between T18 and T25 leading to cAMP synthesis, and transcriptional activation of the lactose or maltose operons that can be easily detected on agar plates. We chose this system because many of the Pil proteins are in the inner membrane and BACTH is particularly appropriate for studying interactions among membrane proteins, as demonstrated by the systematic characterization of the interaction network between proteins involved in cell division in *E. coli* (Karimova *et al.*, 2005). The only limitation of this system is that cAMP needs to be produced in the cytoplasm, precluding the analysis of proteins that have no cytoplasmic domain (*e.g.* proteins localized in the periplasm or outer membrane).

Of the 18 *N. meningitidis* Pil proteins that could be analyzed by BACTH (the localization of PilC1/PilC2, PilP, PilQ and PilW preclude their analysis), we selected 11 (PilD, PilE, PilF, PilG, PilM, PilN, PilO, PilT, PilT2, PilU and PilZ) for a systematic identification of their binary interactions. For each protein, four different plasmids were generated by cloning the full-length corresponding gene into appropriate BACTH vectors to create fusions with the N- or C-termini of T18 and T25. The nomenclature that was used directly reflects the nature of the engineered fusion, *e.g*. T18-PilD and PilD-T18 indicate that the T18 domain has been

fused to the N- and C-terminus of PilD, respectively. All the possible pairs of T18 and T25 plasmids, 484 in total, were co-transformed in BTH101, an *E. coli cya* mutant. Functional complementation between T18 and T25 was determined by plating transformants on selective MacConkey/maltose plates and observing the coloration of the colonies after 40-48 hours of growth at 30°C. In the absence of functional complementation between T18 and T25 the colonies are white, while they are pink when functional complementation occurs. As negative and positive controls, we used BTH101 cells co-transformed with pUT18C/pKT25 plasmids containing no inserts, and pUT18C-zip/pKT25-zip in which T18 and T25 are fused to a 35 aa-long leucine zipper derived from yeast protein GCN4, respectively (Karimova *et al.*, 1998).

Out of the 483 T18/T25 plasmid combinations that could be scored (the PilT2-T18/PilT2-T25 combination was apparently, and for an unknown reason, toxic, and could not be scored as it yielded microscopic colonies even after prolonged incubation), 45 (9.3%) yielded coloured colonies (Figure 1) with coloration varying between light pink and purple. In 11/45 cases (24.4%), only a fraction of the colonies were coloured. Importantly, only one protein (PilD) yielded no interactions, which might be due to its topology. Another advantage of BACTH is that the efficiency of the functional complementation between T18 and T25 can be quantified by measuring β-galactosidase activities in liquid culture (Karimova *et al.*, 1998; Karimova *et al.*, 2005). We therefore quantified the β-galactosidase activity/mg of bacteria (dry weight) harbouring the 45 positive plasmid combinations (Figure 2). Only two combinations, PilM-T18/T25-PilT and T18-PilN/T25-PilT, yielded β-galactosidase activities below the background level measured in the negative control (205 ± 47 U/mg). It is worth noting that in these combinations, only a fraction of the colonies were pink (Figure 1). The β-galactosidase activities for the other combinations ranged between 7,910 ± 262 U/mg for T18-PilT2/T25-PilT2 (which is higher than the activity measured for the positive control, 5,247 ± 1,339 U/mg) and 483 ± 28 U/mg for T18-PilM/T25-PilN (which is more

than two-fold higher than the activity measured for the negative control). Twenty-nine interactions were provisionally classified as strong (β-galactosidase activity > 1,000 U/mg), while 14 were weaker.

In summary, we have identified 43 interactions between 10 Pil proteins using BACTH. Since some interactions were identified mutliple times (*e.g*. the PilZ-PilF interaction has been identified with six different plasmid combinations), this analysis identified 20 different Pil-Pil interactions and outlines the most complex interaction network between Pil proteins to date. A graphical representation of the topology of this network (Figure 2 inset) reveals interesting features. It appears that there are two sub-complexes that are linked through the PilT2-PilG interaction. The first sub-complex consists of the four traffic ATPases (PilF, PilT, PilT2 and PilU) and PilZ that specifically interacts with PilF. The possibility that traffic ATPases form hetero-multimers might have important implications for Tfp biology. The second sub-complex consists almost exclusively of proteins that are thought to be involved in pilus assembly (only PilG acts after that step (Carbonnelle *et al.*, 2006)), which interact in a highly ordered fashion: PilM-PilN-PilO-PilE. Since little is known about the molecular mechanisms of pilus assembly, we focused our further analysis on this sub-complex.

Determination of the membrane topology of PilN and PilO

To better understand the topology of the sub-machinery involved in pilus assembly, it is necessary to know the topology of each of its components. Since the topology of PilE is known (*i.e*. when not part of a pilus, PilE is a bitopic inner membrane protein with its C-terminal globular head in the periplasm) and PilM is cytoplasmic, it was necessary to experimentally determine the topology of PilN and PilO. Indeed, although all bioinformatic tools we have tested agree that these proteins have one transmembrane domain and are therefore bitopic proteins in the inner membrane, they predict different topologies (data not shown). We therefore experimentally determined the membrane topology of PilN and PilO

using a dual reporter *pho-lac* system (Karimova *et al.*, 2009). The full-length *pilN* and *pilO* genes were cloned in frame with a dual reporter encoding an *E. coli* alkaline phosphatase fragment ($PhoA_{22-472}$) and the α-peptide of *E. coli* β-galactosidase ($LacZ_{4-60}$). After introducing the resulting plasmids into *E. coli* DH5α, transformants were streaked on agar plates containing the chromogenic substrate of alkaline phosphatase, X-Phos. A periplasmic location of the reporter is revealed by high alkaline phosphatase activity and hence blue colour, whereas a cytosolic location results in no coloration. As controls directing the reporter to the periplasm or the cytoplasm we used two previously published fusions with the *E.coli* YmgF polytopic protein (Karimova *et al.*, 2009). As can be seen in Figure 3A, both PilN-PhoLac and PilO-PhoLac exhibited a blue phenotype, indicating a periplasmic location of the reporter and hence of the C-terminus of PilN and PilO. $PilN_{1-50}$-PhoLac and $PilO_{1-50}$-PhoLac, in which the reporter was fused with the first 50 residues in both PilN and PilO (that encompass the predicted transmembrane segment) gave similar results (Figure 3A). This confirms that PilN and PilO have a similar topology (Figure 3B). Based on our results and TMHMM predictions (Krogh *et al.*, 2001), PilN and PilO have a short N-terminal segment of 20-27 aa in the cytoplasm, one transmembrane helix and the C-terminal main part of the protein (154 of 199 aa for PilN and 174 of 215 aa for PilO) in the periplasm.

Mapping of the interaction domains between PilE, PilM, PilN and PilO

Next, we further examined the interactions between PilE, PilM, PilN and PilO by mapping the domains critical for protein-protein interaction using BACTH. We generated truncated versions of PilE, PilN and PilO corresponding to the first 39 to 50 residues of these proteins ($PilE_{1-39}$, $PilN_{1-50}$ and $PilO_{1-50}$), which consist mainly of the short cytoplasmic domain and the transmembrane helix. Our rationale was that this would help determine the contribution of the C-terminal periplasmic domains of these proteins to the interactions identified above. These shorter versions were fused to T18 and T25 as above and the corresponding

plasmids were then co-transformed in *E. coli* BTH101. Functional complementation between T18 and T25 was further quantified by measuring β-galactosidase activities in liquid culture (Figure 4).

The first interaction we examined was PilM-PilN, which was identified in two combinations (T18-PilM/T25-PilN and T18-PilN/T25-PilM). Due to the topology of PilN (Figure 3B) and the cytoplasmic localization of PilM, it was expected that the interaction between these two proteins would rely on the short cytoplasmic fragment of PilN. Our analysis showed that $PilN_{1-50}$ interacts with PilM as well as the full-length version of this protein (Figure 4), and this was observed in both the above combinations. Interestingly, for a reason that remains unknown, the T18-PilM/T25-$PilN_{1-50}$ interaction (787 ± 112 U/mg) was even slightly stronger than the original T18-PilM/T25-PilN (450 ± 13 U/mg). These results demonstrate that PilM interacts with the N-terminus of PilN, which is the only domain of this latter protein critical for the interaction.

Next, we examined the PilN-PilO interaction, which was also identified in two combinations (T18-PilO/T25-PilN and T18-PilN/T25-PilO). Unlike T18-$PilO_{1-50}$/T25-PilN, in which there was no functional complementation between T18 and T25, the T18-PilO/T25-$PilN_{1-50}$ combination yielded significant β-galactosidase activity (609 ± 36 U/mg) that was approx. five times higher than the negative control (127 ± 25 U/mg) (Figure 4). However, this activity was reduced when compared to that of the original T18-PilO/T25-PilN (1,049 ± 129 U/mg). In the second combination, T18-PilN/T25-PilO, functional complementation between T18 and T25 was abolished with shorter versions of the proteins. Taken together, these results indicate that the PilN-PilO interaction relies mainly on the globular periplasmic domains of these proteins, but that the N-terminus of PilN contributes to this interaction since T25-$PilN_{1-50}$ was still capable of interacting with T18-PilO.

Finally, we examined the PilO-PilE interaction, which was again identified in two combinations (T18-PilO/T25-PilE and T18-PilE/T25-PilO). In the first combination, T18-

PilO/T25-PilE, no functional complementation between T18 and T25 was detected with shorter versions of the proteins. In the second combination, while no functional complementation occured with T18-PilE/T25-PilO$_{1-50}$, the T18-PilE$_{1-39}$/T25-PilO plasmids yielded significant β-galactosidase activity (493 ± 89 U/mg) (Figure 4). However, this activity was approx. three times lower than that measured with full-length proteins T18-PilE/T25-PilO (1,448 ± 350 U/mg). These results indicate that the PilO-PilE interaction is mediated mainly by the globular periplasmic domains of these proteins, but that the N-terminus of PilE contributes to this interaction since T18-PilE$_{1-39}$ was capable of interacting with T25-PilO.

Taken together, these results give a clear picture of the topology of the sub-complex involved in Tfp assembly. In brief, PilM interacts with the N-terminus of PilN, which interacts with PilO along the whole length of the two proteins. PilO then interacts with PilE along the whole length of the two proteins.

Assessment of the functional importance of a conserved N-terminal motif in PilN

As described previously (Sampaleanu *et al.*, 2009; Karuppiah and Derrick, 2011), the cytoplasmic portion of PilN contains a short motif INLLPY (residues 7 to 12) that is highly conserved even in phylogenetically distant species, which suggests that it could be functionally important. Since we found that the cytoplasmic portion of PilN is critical for the interaction between PilM and PilN (see Figure 4), we postulated that the INLLPY motif might play a role in this interaction. This was tested by constructing variants of PilN in which three invariant residues in the above motif were individually changed to alanines by site-directed mutagenesis (PilN$_{N8A}$, PilN$_{L9A}$ and PilN$_{P11A}$) and the effect on the functional complementation between T18 and T25 observed in the T18-PilM/T25-PilN and T18-PilN/T25-PilM combinations was quantified by measuring the corresponding β-galactosidase activities (Figure 5A). In both combinations, no functional complementation occurred with the

279 $PilN_{N8A}$ and $PilN_{L9A}$ variants, while the $PilN_{P11A}$ variant was still able to interact with PilM as
280 well as $PilN_{WT}$ (Figure 5A). Importantly, the absence of functional complementation with the
281 $PilN_{N8A}$ and $PilN_{L9A}$ variants was not due to a lack of production and/or major instability since
282 these variants were able to interact with PilO in the T18-PilO/T25-PilN and T18-PilN/T25-
283 PilO combinations (Figure 5A) and were expressed as well as $PilN_{WT}$ as demonstrated by
284 immunoblotting (data not shown). It should be noted, however, that the β-galactosidase
285 activities with the $PilN_{N8A}$ variant were reduced when compared to that measured with $PilN_{WT}$
286 (456 ± 29 U/mg versus 1,212 ± 468 U/mg in the T18-PilO/T25-PilN combination, and 439
287 ± 36 U/mg versus 1,049 ± 114 U/mg in the T18-PilN/T25-PilO combination), which
288 suggests that the N-terminus of PilN might also play a small role in the PilN-PilO interaction.
289 Next, we tested whether these PilN variants were functional in *N. meningitidis* by
290 assessing whether they were able to restore piliation in a *pilN* mutant. The different *pilN*
291 alleles constructed by site-directed mutagenesis were cloned under the control of an IPTG-
292 inducible promoter, and they were again demonstrated by immunoblotting to be expressed
293 as well as $PilN_{WT}$ (data not shown), and integrated ectopically in the genome of a non polar
294 *ΔpilN* meningococcal mutant. Piliation in the presence of IPTG was then assessed by
295 immunofluorescence (IF) microscopy, using the 20D9 monoclonal antibody that is specific
296 for the Tfp of strain 8013 (Pujol *et al.*, 1997). As can be seen in Figure 5B, piliation was
297 restored in the *ΔpilN/pilN*$_{P11A}$ strain at levels indistinguishable from those observed in the
298 *ΔpilN/pilN*$_{WT}$ complemented mutant, which indicates that $PilN_{P11A}$ is functional with respect to
299 Tfp biogenesis. In contrast, the *ΔpilN/pilN*$_{N8A}$ and *ΔpilN/pilN*$_{L9A}$ strains are non-piliated, even
300 though they produce the corresponding PilN variants as verified by immunoblotting (data not
301 shown), indicating that $PilN_{N8A}$ and $PilN_{L9A}$ are unable to promote Tfp biogenesis.
302 Taken together, these data confirm that the highly conserved N-terminal motif in PilN is
303 crucial for this protein's function, most probably by mediating the PilM-PilN interaction within
304 the sub-complex involved in pilus assembly.

Further characterization of a complex between PilM, PilN, PilO and PilP

As mentioned above, one of the proteins predicted to be involved in pilus assembly, PilP (Carbonnelle *et al.*, 2006), could not be analyzed using BACTH because it is a lipoprotein that does not possess a cytoplasmic portion (Golovanov *et al.*, 2006). Therefore, to further improve our understanding of the composition of the pilus assembly machinery, we decided to test interactions between PilP and the PilM, PilN and PilO proteins by determining (by immunoblotting) the stability of every protein in *N. meningitidis* non polar deletion mutants in each corresponding gene and by using a biochemical approach, *i.e*. by performing co-immunoprecipitations.

We first generated rabbit antisera for these four proteins and used them to confirm that PilM, PilN, PilO and PilP were detected by immunoblotting in the WT strain and not in non polar mutants in which the respective genes were cleanly deleted (Figure 6A). As previously done in EPEC or *P. aeruginosa* (Ramer *et al.*, 2002; Ayers *et al.*, 2009), we performed further immunoblots to determine whether deletion of one of the above four proteins had a negative impact on the stability of the remaining three, which is considered as evidence that these proteins form a complex. As shown in Figure 6A, while PilM levels were unaffected by the absence of and PilM had no impact on the levels of PilN, PilO and PilP, the latter three proteins showed mutually stabilizing effects. PilN and PilO were strongly dependent on each other for stability and the absence of either protein resulted in slightly reduced levels of PilP. In the absence of PilP, there was a dramatic decrease of levels of both PilN and PilO. We ruled out the possibility that the above effects were due to polarity since in each case stability of each protein was restored in complemented mutants in which a WT copy of the corresponding genes was expressed ectopically under the transcriptional control of an IPTG-inducible promoter (Figure 6A).

Since most of the above proteins are membrane proteins, we performed protein extraction using B-PER that contains a mild, non-ionic detergent. After cross-linking of the antibodies against PilM, PilN, PilO and PilP to protein A/G agarose, identical amounts of B-PER protein extracts were subjected to immunoprecipitations. Each antibody could immunoprecipitate the corresponding protein from the WT strain but not from mutants in which the respective genes were interrupted (data not shown). Precipitated samples were then subjected to immunobloting using the PilP anti-serum. As shown in Figure 6B, PilP co-immunoprecipitates with PilM, PilN and PilO when using the antibodies raised againts these proteins. Control experiments showed that PilP was not precipitated with the same antibodies when using B-PER extracts prepared from *ΔpilM*, *ΔpilN*, *ΔpilO* and *ΔpilP* mutants (Figure 6B). These results show that the PilM, PilN, PilO and PilP proteins involved in pilus assembly form a multi-molecular sub-complex in the inner membrane of *N. meningitidis*.

Next, we tested whether this sub-complex, that probably represents the core pilus assembly machinery, could form in the absence of other Pil proteins. To achieve this, we first constructed an *E. coli* strain in which PilM, PilN, PilO and PilP were co-expressed. Expression of the four proteins was confirmed by immunoblotting using the above antibodies (data not shown). After extracting proteins with B-PER, we performed immunoprecipitations as above with the antibodies against PilM, PilN, PilO and PilP, respectively. We confirmed as above that each antibody could immunoprecipitate the corresponding protein (data not shown). Precipitated samples were then subjected to immunobloting using the anti-PilP serum. As shown in Figure 6C, PilM, PilN, PilO and PilP proteins could be co-immunoprecipitated when co-expressed in *E. coli*.

Taken together, these results suggest that the widely conserved PilM, PilN, PilO and PilP proteins that are dedicated to assembly of pilus filaments can form a complex in the meningococcus. No other Pil proteins are necessary for this complex to form as it can be detected in *E. coli* by co-expressing only the *pilM*, *pilN*, *pilO* and *pilP* genes.

Discussion

Now that all the genes involved in Tfp biology have been identified and the corresponding mutants systematically characterized, the next step to better understanding of the mechanisms governing the assembly and functionality of these widespread virulence organelles is defining the way the numerous corresponding proteins interact to form what is expected to be an intricate machinery.

Large-scale studies of interactions between proteins involved in Tfp biology have only been performed in the Tfpb-expressing organism EPEC. Similar studies have also been performed for the evolutionarily related type II secretion machinery (Ayers *et al.*, 2010). In EPEC, using comprehensive collections of in-frame deletion mutants and antibodies against the corresponding proteins, Ramer *et al*. found that the stability of 11 of the 12 Bfp proteins necessary for pilus biogenesis depends on the presence of at least one other Bfp proteins, which was taken as (indirect) evidence that these proteins interact (Ramer *et al.*, 2002). Together with the experimental localization of these proteins in different cellular fractions, it was inferred that two topographically distinct sub-complexes exist: one in the outer membrane centered on the secretin multimers that serve as a channel for the growing Tfp, and one at the inner membrane consisting of the pilin, pilin-like proteins and inner membrane proteins. Direct evidence that at least 10 of these Bfp proteins physically interact was obtained by immunoblotting after affinity purification of a chemically cross-linked oligomeric protein complex (Hwang *et al.*, 2003). Unfortunately, owing to the extensive differences between the two Tfp subtypes (Pelicic, 2008), these results cannot be easily extrapolated to Tfpa-expressing bacteria that represent the vast majority of the bacteria that harbour Tfp. This prompted us to initiate this large-scale identification of the binary interactions (which remain for the most part uncharted in the above studies) between Tfpa Pil proteins using the human pathogen *N. meningitidis* as a model. We opted for BACTH

because it has proven invaluable for the study of complex membrane-localized protein machineries (Karimova *et al.*, 2005).

We decided to focus our efforts on the putative sub-complex at the inner membrane where most of the divergence between Tfpa and Tfpb systems reside (Pelicic, 2008). Of the 18 proteins having a predicted topology *a priori* compatible with BACTH analysis, we selected 11, including six out seven proteins (PilD, PilE, PilF, PilM, PilN and PilO) predicted to be essential for pilus assembly (Carbonnelle *et al.*, 2006), all the traffic ATPases (PilF, PilT, PilT2 and PilU), the universally conserved inner membrane protein PilG and a cytoplasmic protein of unclear function (PilZ). Strikingly, only the prepilin peptidase PilD yielded no interactions, which is perhaps surprising given its role in processing the leader peptide of prepilins and prepilin-like proteins (Strom *et al.*, 1993). However, a subsequent prediction of its topology by TMHMM (Krogh *et al.*, 2001) indicates that this is most likely because both the N- and C-terminus of PilD, to which the T18 and T25 fragments have been fused, might be on the periplasmic side of the inner membrane and therefore incompatible with BACTH analysis. Therefore, if this BACTH analysis is to be extended in the future to the remaining seven pilin-like proteins (ComP, PilH, PilI, PilJ, PilK, PilV and PilX), PilD should be excluded. Nevertheless, since each studied gene is cloned in four different vectors, this would still represent a very substantial effort with the testing of 756 additional combinations of T18 and T25 plasmids.

The first important finding in this study, which identified the largest interaction network between proteins involved in Tfp biology, is that multiple interactions occured between the four traffic ATPases present in the meningococcus. Traffic ATPases, which have been extensively studied, form toroidal homohexamers that convert the energy from ATP hydrolysis into mechanical energy (Satyshur *et al.*, 2007; Savvides, 2007), which in Tfp biology is used to power pilus assembly (PilF) or retraction (PilT). Therefore, the homotypic PilF-PilF and PilT-PilT interactions were not unexpected, and the PilT2-PilT2 interactions

suggest that this recently discovered paralog of PilT (Brown *et al.*, 2010) might form hexamers as well. The reason we did not identify PilU-PilU interactions is unclear at this time. Strikingly, we found evidence that different traffic ATPases interact with each other as evidenced by the PilF-PilT2, PilT-PilT2, PilU-PilT and PilU-PilT2 interactions. PilT2 appears to be a hub as it interacts with all the other traffic ATPases. Although a higher order interaction between different homo-hexamers cannot be excluded, it is possible that hetero-hexamers exist (Figure 7). Such hetero-hexamers could have important roles in Tfp biology. For example, it is possible that pilus retraction is fine-tuned by PilT-PilT2, PilT-PilU and PilT-PilT2-PilU hetero-hexamers, which would strengthen our earlier assumption that PilT paralogs in the meningococcus are unlikely to form separate retraction motors based on the finding that when overexpressed PilT2 and PilU cannot substitute for PilT (Brown *et al.*, 2010). Furthermore, such a possibility is consistent with the phenotypic defects in meningococcal *pilT2* and *pilU* mutants that were suggested to result from altered pilus dynamics (Brown *et al.*, 2010). Another important player in this fine-tuning of pilus dynamics might be PilZ, which is dispensable for piliation in the meningococcus but plays an important role in Tfp biology (Brown *et al.*, 2010), that interacts strongly and specifically with PilF. These findings strengthen a previous report describing an interaction between the PilZ and PilF orthologs in *Xanthonomas campestris* (Guzzo *et al.*, 2009). Hetero-hexamers of traffic ATPases might also provide an elegant explanation to the question of how bacteria can switch between pilus extension and retraction. Rather than two different homo-hexameric motors switching at the base of the pilus, which is hardly compatible with the extremely rapid switches between extension and retraction, there could be a single hetero-hexameric motor the net composition of which could vary and govern extension or retraction of the pilus.

The second important finding in this study was that five out seven proteins that were originally predicted to play a role in pilus assembly based on genetic studies (PilD, PilE, PilF, PilM, PilN, PilO and PilP) (Carbonnelle *et al.*, 2006) indeed form a sub-complex at the inner

membrane. There was only limited evidence for this complex so far in *P. aeruginosa* in which the absence of one of the PilM, PilN, PilO and PilP proteins was shown to have a negative impact on the stability of the others (Ayers *et al.*, 2009). While we now understand why the prepilin peptidase PilD was not found within this complex, this is less clear for PilF which powers pilus assembly. However, several scenarios might explain this apparent incongruity: (i) interaction of PilF with the pilus assembly sub-complex might be too transient to be detected by BACTH, (ii) PilF might interact with PilE only when this protein has been processed by PilD (the full-length prepilin gene has been cloned in BACTH vectors used in this study), or (iii) more than one Pil partner might be necessary for PilF to interact with the pilus assembly sub-complex. We have further unravelled the architecture of the above sub-complex (Figure 7) by using a combination of different approaches. We have found that PilM, an ATP-binding cytoplasmic protein (Karuppiah and Derrick, 2011), interacts with itself and the N-terminus of the bitopic PilN protein that is on the cytoplasmic side of the inner membrane. This interaction is dependent on a short sequence motif in PilN that was found to be very conserved and predicted to be functionally important (Ayers *et al.*, 2009), which we have demonstrated here. Point mutants in this INLLPY motif abolish the PilM-PilN interaction and piliation altogether, which validates the recently reported 3D structure of *Thermus thermophilus* PilM (Karuppiah and Derrick, 2011). Indeed, high quality crystals of PilM could only be obtained in this study in the presence of a synthetic peptide corresponding to the N-terminus of PilN encompassing the above motif. PilN then interacts with the other bitopic inner membrane protein PilO. This interaction relies mainly on the periplasmic domains of these two proteins, which confirms a recent report showing that when co-expressed in *E. coli* the periplasmic domains of *P. aeruginosa* PilN and PilO form a stable hetero-dimer (Sampaleanu *et al.*, 2009). However, we show here that the transmembrane domains of PilN and PilO also contribute to this interaction. Finally PilP, which could not be analyzed by BACTH, was found to interact with PilM-PilN-PilO by showing that the absence of one these

460 proteins often results in instability/degradation of the others and/or by showing that they co-
461 immunoprecipitate. This is an important result as it shows that the above binary BACTH
462 interactions co-exist *in vivo* and lends further support for the existence of a PilM-PilN-PilO-
463 PilP complex. Although it is clear based on their predicted topologies that PilP cannot
464 interact with PilM, its is difficult to predict whether it interacts with PilN, PilO or both proteins
465 (Figure 7). This latter possibility is supported by the dramatically reduced stability of both
466 PilN and PilO in a *ΔpilP* mutant and by a very recent report showing that when a soluble
467 version of *P. aeruginosa* PilP was co-expressed in *E. coli* with the periplasmic domains of
468 PilN and PilO, these proteins proteins formed a stable hetero-trimer (Tammam *et al.*, 2011).
469 Another significant result was that the main pilus constituent, PilE, interacts strongly with
470 PilO (and more weakly with PilN), which provides a snapshot of the sub-complex involved in
471 pilus assembly in the presence of its actual substrate, the pilin.
472 Finally, our findings concerning the universally conserved inner membrane protein PilG
473 whose role in Tfp biology is unclear are also notable. It seems unlikely that PilG is the inner
474 membrane scaffold on which the entire pilus biogenesis protein machinery is built, as often
475 postulated, because it interacts only with 3 proteins (which is less than the number of
476 interactions identified for the PilT2 ATPase that is dispensable for Tfp biogenesis). This is
477 consistent with our prior finding that PilG is dispensable for pilus assembly since a *pilG/T*
478 meningococcal mutant is piliated (Carbonnelle *et al.*, 2006). However, we found that PilG
479 interacts strongly with PilE and PilO that are essential for pilus assembly, which suggests
480 that further studies are needed to determine its exact role in Tfp biology.
481 In summary, our work provides a picture with unprecedented detail of the
482 macromolecular machinery at play in Tfp biology in a model piliated organism, *N.*
483 *meningitidis*. Moreover, by showing that the sub-complex dedicated to pilus assembly can
484 self-assemble in *E. coli*, this study paves the way for a previously unexplored research
485 avenue consisting in the reconstitution of a minimal Tfpa assembly system in this host,

which could have important consequences on our understanding of the biology of these fascinating organelles.

Materials and methods

Strains and plasmids

E. coli DH5α was used for cloning and topology determination experiments. *E. coli* BTH101 (Euromedex), which is a non-reverting *cya* mutant (F-, *cya-99*, *araD139, galE15, galK16, rpsL1*, *hsdR2, mcrA1, mcrB1)*, was used for BACTH assays. *E. coli* BL21(DE3) was used for protein expression and purification experiments. Strains were routinely grown in liquid or solid Luria-Bertani (LB) medium (Difco) containing, when required, 100 μg/ml spectinomycin, 100 μg/ml ampicillin and 50 μg/ml kanamycin (all from Sigma). Ultra-competent cells were prepared as described elsewhere (Inoue *et al.*, 1990). The WT strain of *N. meningitidis* used in this study is a recently sequenced and systematically mutagenized variant of the serogroup C clinical isolate 8013 (Geoffroy *et al.*, 2003; Rusniok *et al.*, 2009). *N. meningitidis* was grown on GCB agar plates (Difco) containing Kellogg's supplements and, when required, 100 μg/ml kanamycin and 3 μg/ml erythromycin. Plates were incubated in a moist atmosphere containing 5% CO_2.

The plasmids used for BACTH assays were constructed as follows. The full-length *pilD*, *pilE*, *pilF*, *pilG*, *pilM*, *pilN*, *pilO*, *pilT*, *pilT2*, *pilU* and *pilZ* genes were amplified from strain 8013 genomic DNA (extracted with the Wizard genomic DNA purification kit from Promega) using *Pfu*Ultra II DNA polymerase (Agilent) and suitable primers (Table 1). PCR products were cloned directly in pCR8/GW/TOPO (Invitrogen) (Table 2). All the inserts were verified by sequencing to contain no errors. Each *pil gene* was then gel-extracted (using NucleoSpin Extract II from Macherey-Nagel) after *Bam*HI and *Kpn*I digestion and sub-cloned into each BACTH vector (pUT18, pUT18C, pKT25 and pKNT25) cut with the same enzymes (Table 2). The same two-step cloning strategy was used to produce BACTH plasmids in which truncated versions of *pilE*, *pilN* and *pilO* amplified using suitable primers (Table 1) were fused to T18 and T25 (Table 2).

pKTop, which contains a dual reporter *pho-lac* (Karimova *et al.*, 2009), was used to determine the topology of PilN and PilO. Full-length or truncated versions of the *pilN* and *pilO* genes have been gel-extracted after *Bam*HI and *Kpn*I digestion of the corresponding pCR8/GW/TOPO derivatives and sub-cloned into pKTop cut with the same enzymes (Table 2). The *pil* gene were thus fused in frame with the dual reporter. The resulting recombinant plasmids were transformed into competent *E. coli* DH5α cells, which were plated on LB plates supplemented with 80 μg/ml of X-phos (5-bromo-4-chloro-3-indolyl phosphate disodium salt) (Sigma), 1 mM IPTG (isopropyl-β-D-thiogalactopyranoside) (Merck Chemicals), 50 mM phosphate buffer (pH 7.0), and 50 μg/ml kanamycin. The plates were incubated overnight at 37°C and the coloration was scored.

pilN point mutant alleles were generated using the Quickchange site-directed mutagenesis kit (Stratagene) as previously described (Helaine *et al.*, 2007), with pYU61 used as DNA template and a series of complementary primers (Table 1). All mutant *pilN* alleles have been verified by sequencing before they were sub-cloned into BACTH vectors as above. The *pilN* mutant alleles were also amplified using suitable primers flanked by *Pac*I sites and sub-cloned in pGCC4 (Mehr *et al.*, 2000) restricted with the same enzyme. This generated vectors that contain the mutant alleles under the transcriptional control of an IPTG-inducible promoter within a region of the gonococcal genome conserved in *N. meningitidis*. These vectors were first transformed into strain 8013 in which genome they integrated by allelic exchange, and the endogenous *pilN* copy was then interrupted by transforming these strains with genomic DNA extracted from a *ΔpilN* non polar mutant (see below). The resulting strains were grown on GCB agar plates supplemented with 100 μg/ml kanamycin, 3 μg/ml erythromycin and 0.25 mM IPTG before they were analyzed for piliation as described below. *N. meningitidis* non polar *ΔpilM*, *ΔpilN*, *ΔpilO* and *ΔpilP* mutants have been constucted by splicing PCR as described elsewhere (de Berardinis *et al.*, 2008). In brief, two sets of primers (F1/R1 and F2/R2) were used to amplify approx. 500 bp fragments

upstream and downstream from each target gene, respectively. The R1 and F2 primers were designed to delete the coding region of the mutagenized genes from the start codon to approx. 30 bp before the stop codon in order to preserve ribosomal binding sites used by downstream genes. Primers R1 and F2 contained 23-mer overhangs that are complementary to the aphF and aphR primers used to amplify the promoterless *aphA-3* antibiotic selection cassette from start to stop codons, respectively. Primers F1 and/or R2 contained 12-mer overhangs corresponding to the DNA uptake sequence that is necessary for DNA to be taken up by the meningococcus during natural transformation. In the first step, three PCR fragments were amplified using F1/R1, F2/R2 and aphF/aphR, and the high-fidelity Herculase II Fusion DNA polymerase (Agilent). These fragments were then combined and spliced together using the same enzyme and the F1 and R2 primers. The spliced PCR fragments were then directly transformed into *N. meningitidis* and mutants were selected on GCB agar plates supplemented with 100 μg/ml kanamycin. For each mutant, at least two colonies were isolated and further verified by PCR using the F1 and R2 primers. These mutations were then transformed into strains in which genome the WT alleles under the transcriptional control of an IPTG-inducible promoter were previously integrated by allelic exchange (Carbonnelle *et al.*, 2006).

To produce and/or purify antibodies against PilM, PilN, PilO and PilP (see below), we constructed a series of plasmids for expressing these proteins in *E. coli*. First, two plasmids designed to produce PilM and PilP fused to a polyhistidine-tag were constructed as follows. Full-length *pilM* was amplified using suitable primers (Table 1) and cloned directly in pCRII-TOPO (Invitrogen). The *pilM* insert, which was verified by sequencing to contain no errors, was then gel-extracted after *Nde*I and *Bam*HI digestion and sub-cloned in pET-14b cut with the same enzymes (Table 2). An internal fragment of the *pilP* gene (coding for residues 17-145 of the mature protein) was also cloned using a similar two-step cloning strategy in pET-20b cut with *Eco*RI and *Xho*I. Subsequently, to increase protein yields during purification, we

567 designed a series of plasmids to produce PilM, PilN and PilO fused to the maltose-binding
568 protein (MBP). The full-length genes were amplified using suitable primers (Table 1), cloned
569 in pCR8/GW/TOPO and found to contain no errors by sequencing (Table 2). They were then
570 gel-extracted after *Eco*RI and *Sal*I (*pilM*), *Eco*RI and *Pst*I (*pilN*), or *Eco*RI and *Pst*I (*pilO*)
571 digestions and sub-cloned in the pMAL-c2x vector cut with the same enzymes (Table 2).
572 To engineer an *E. coli* strain that co-expresses PilM, PilN, PilO and PilP, we amplified
573 the entire locus from strain 8013 using suitable primers (Table 1), gel-extracted it after *Nde*I
574 and *Xho*I digestion and cloned it directly in pACYCDuet-1 vector (Novagen) cut with the
575 same enzymes (Table 2).
576
577 ***BACTH procedures***
578 Competent BTH101 cells were co-transformed with 20 ng each of two recombinant plasmids
579 encoding fusions to T18 and T25, respectively. Two hundred µl of the transformed cells was
580 plated on MacConkey agar base medium supplemented with 0.5 mM IPTG, 1% maltose
581 solution (Sigma), 100 µg/ml ampicillin and 50 µg/ml kanamycin. Plates were incubated at
582 30°C and the color of the colonies was scored after 40-48 h. In every assay, positive and
583 negative controls, generating purple and white colonies respectively, were included. All the
584 positive plasmid combinations, *i.e*. generating coloured colonies, were transformed again for
585 confirmation of the phenotypes.
586 The efficiency of the functional complementation between T18 and T25 for the positive
587 plasmid combinations, were quantified by measuring β-galactosidase activities in liquid
588 culture (Karimova *et al.*, 1998). Transformants to be assayed were grown at 30°C for 14-16
589 h in 5 ml of LB supplemented with 0.5 mM IPTG, 100 µg/ml ampicillin and 50 µg/ml
590 kanamycin. At least three independent cultures were performed for each transformant to be
591 tested. These were then diluted 1/5 in M63 broth and the OD_{600} was recorded. Next, cells
592 were permeabilized by adding 20 µl of chloroform and 20 µl of 0.1% SDS to 1.5 ml of

bacterial suspension. Tubes were then subjected to vortexing for 10 sec and incubated at 37°C in a shaking incubator for 40 min. For the enzymatic reactions, 10 µl of the permeabilized cells were added to 990 µl of PM2 (70 mM $Na_2HPO_4.12H_2O$, 30 mM NaH_2PO_4 H_2O, 1 mM $MgSO_4$, 0.2 mM $MnSO_4$, pH 7.0) containing 100 mM β-mercaptoethanol. The tubes were placed in a heat block at 28°C for 5 min before the reaction was started by adding 0.25 ml of 0.4% O-nitrophenol-β-galactoside (ONPG) in PM2 buffer (without β-mercaptoethanol). The reaction was stopped by the addition of 0.5 ml of 1 M Na_2CO_3, which occurred after 20 min for positive samples and after 60 min for negative samples, at which point the OD_{420} and OD_{600} were recorded. The enzymatic activity A (in units/ml) was calculated using the following formula: A = 200 x (OD_{420}/min of incubation) x dilution factor. The results were expressed as units of enzymatic activity per mg of bacterial dry weight, where 1 unit corresponds to 1 nmol of ONPG hydrolyzed per min (Karimova *et al.*, 1998), considering that 1 ml of culture at and OD_{600} of 1 corresponds to 300 µg bacteria (dry weight).

SDS-PAGE, antisera and immunoblotting

N. meningitidis whole-cell protein extracts were prepared as previously described (Helaine *et al.*, 2005) or by resuspending bacteria directly in Laemmli sample buffer (Bio-Rad) and heating for 10 min at 100ºC. *E. coli* whole-cell protein extracts were prepared by centrifuging bacteria and resuspending pellets directly in Laemmli sample buffer. When needed, proteins were quantified using the Bio-Rad Protein Assay as suggested by the manufacturer. Separation of the proteins by SDS-PAGE and subsequent blotting to Amersham Hybond ECL membranes (GE Healthcare) was done using standard molecular biology techniques (Sambrook and Russell, 2001). Blocking, incubation with primary and/or secondary antibodies and detection using Amersham ECL Plus (GE Healthcare) were done following the manufacturer's instructions. Alternatively, SDS-PAGE gels were stained using Bio-Safe

619 Coomassie stain (Bio-Rad). Rabbit antisera were used at 1/2,000 (anti-PilO), 1/5,000 (anti-
620 PilM and anti-PilN) and 1/50,000 (anti-PilP) dilutions. Amersham ECL-HRP linked secondary
621 anti-rabit antibody (GE Healthcare) was used at a 1/10,000 dilution.
622 Antisera against PilM, PilN, PilO and PilP were produced in rabbits as follows. Two
623 antisera (anti-PilM and anti-PilP) were produced against purified recombinant proteins. Anti-
624 PilM was produced against a recombinant polyhistidine-PilM (full-length protein) that was
625 purified from *E. coli* BL21 (pYU12) using Ni-NTA affinity resin (Qiagen). Anti-PilP was
626 produced against a recombinant $PilP_{17-145}$-polyhistidine that was purified from *E. coli* BL21
627 (pET20-*pilP*) using Ni-NTA affinity resin. Anti-PilN and anti-PilO were produced by
628 immunizing animals with a mixture of two different peptides from the same antigen using the
629 Double-X strategy (Eurogentec). Peptides corresponding to residues 125-140 and 185-199
630 of PilN, and 45-59 and 169-183 of PilO were used for the immunizations. Anti-PilM, anti-PilN
631 and anti-PilO sera have been purified by immuno-affinity using MBP-PilM, MBP-PilN and
632 MBP-PilO recombinant proteins that were purified using amylose resin (New England
633 Biolabs) from *E. coli* BL21 transformed with pYU42, pYU51 and pYU44, respectively.
634
635 ***Detection of Tfp***
636 Tfp were visualized by IF microscopy using a Nikon Eclipse E600 microscope as previously
637 described (Helaine *et al.*, 2005). The only minor differences consisted in the use of DAPI
638 (4′,6-diamidino-2-phenylindol) (Invitrogen) at 100 ng/ml for staining the bacteria, and the use
639 of Aqua-Poly/Mount (Polysciences, Inc.) as mounting medium.
640
641 ***Immunoprecipitations***
642 Immunoprecipitations were performed using the Crosslink immunoprecipitation kit (Pierce)
643 following the manufacturer's instructions. In brief, antibodies were first bound to Protein A/G
644 Plus Agarose (5 µg of purified anti-PilM, anti-PilN and anti PilO antibodies, and 8 µl of anti-

PilP serum) and then cross-linked using dissuccinimidyl suberate (DSS). Protein extracts, prepared using the B-PER bacterial protein extraction reagent (Pierce), were then immunoprecipitated (500 µg/reaction) overnight at 4ºC. After several washing steps, precipitated proteins were eluted in 50 µl of elution buffer and analyzed by immunoblotting as described above.

Acknowledgements

This work was supported by grants from the Biotechnology and Biological Sciences Research Council (BBSRC) and European Commission (EIMID, Seventh Framework Programme). M. Georgiadou was supported by a Doctoral Training Grant fom the BBSRC. We thank E. Carbonnelle (Hôpital Européen Georges-Pompidou) for help with production of anti-PilP antibody. We are grateful to C. M. Tang (Oxford University) for critical reading of this manuscript.

659 **References**

660 Ayers, M., Howell, P.L. and Burrows, L.L. (2010) Architecture of the type II secretion and
661 type IV pilus machineries. *Future Microbiol* **5**: 1203-1218.

662 Ayers, M., Sampaleanu, L.M., Tammam, S., Koo, J., Harvey, H., Howell, P.L. and Burrows,
663 L.L. (2009) PilM/N/O/P proteins form an inner membrane complex that affects the stability
664 of the *Pseudomonas aeruginosa* type IV pilus secretin. *J Mol Biol* **394**: 128-142.

665 Brown, D., Helaine, S., Carbonnelle, E. and Pelicic, V. (2010) Systematic functional analysis
666 reveals that a set of 7 genes is involved in fine tuning of the multiple functions mediated
667 by type IV pili in *Neisseria meningitidis*. *Infect Immun* **78**: 3053-3063.

668 Carbonnelle, E., Helaine, S., Nassif, X. and Pelicic, V. (2006) A systematic genetic analysis
669 in *Neisseria meningitidis* defines the Pil proteins required for assembly, functionality,
670 stabilization and export of type IV pili. *Mol Microbiol* **61**: 1510-1522.

671 Carbonnelle, E., Helaine, S., Prouvensier, L., Nassif, X. and Pelicic, V. (2005) Type IV pilus
672 biogenesis in *Neisseria meningitidis*: PilW is involved in a step occuring after pilus
673 assembly, essential for fiber stability and function. *Mol Microbiol* **55**: 54-64.

674 Craig, L. and Li, J. (2008) Type IV pili: paradoxes in form and function. *Curr Opin Struct Biol*
675 **18**: 267-277.

676 Craig, L., Pique, M.E. and Tainer, J.A. (2004) Type IV pilus structure and bacterial
677 pathogenicity. *Nat Rev Microbiol* **2**: 363-378.

678 de Berardinis, V.*, et al.* (2008) A complete collection of single-gene deletion mutants of
679 *Acinetobacter baylyi* ADP1. *Mol Syst Biol* **4**: 174.

680 Geoffroy, M., Floquet, S., Métais, A., Nassif, X. and Pelicic, V. (2003) Large-scale analysis
681 of the meningococcus genome by gene disruption: resistance to complement-mediated
682 lysis. *Genome Res* **13**: 391-398.

683 Golovanov, A.P.*, et al.* (2006) The solution structure of a domain from the *Neisseria*
684 *meningitidis* lipoprotein PilP reveals a new ß-sandwich fold. *J Mol Biol* **364**: 186-195.

685 Guzzo, C.R., Salinas, R.K., Andrade, M.O. and Farah, C.S. (2009) PilZ protein structure and
686 interactions with PilB and the FimX EAL domain: implications for control of type IV pilus
687 biogenesis. *J Mol Biol* **393**: 848-866.
688 Helaine, S., Carbonnelle, E., Prouvensier, L., Beretti, J.-L., Nassif, X. and Pelicic, V. (2005)
689 PilX, a pilus-associated protein essential for bacterial aggregation, is a key to pilus-
690 facilitated attachment of *Neisseria meningitidis* to human cells. *Mol Microbiol* **55**: 65-77.
691 Helaine, S., Dyer, D.H., Nassif, X., Pelicic, V. and Forest, K.T. (2007) 3D structure/function
692 analysis of PilX reveals how minor pilins can modulate the virulence properties of type IV
693 pili. *Proc Natl Acad Sci USA* **104**: 15888-15893.
694 Hwang, J., Bieber, D., Ramer, S.W., Wu, C.Y. and Schoolnik, G.K. (2003) Structural and
695 topographical studies of the type IV bundle-forming pilus assembly complex of
696 enteropathogenic *Escherichia coli*. *J Bacteriol* **185**: 6695-6701.
697 Inoue, H., Nojima, H. and Okayama, H. (1990) High efficiency transformation of *Escherichia*
698 *coli* with plasmids. *Gene* **96**: 23-28.
699 Karimova, G., Dautin, N. and Ladant, D. (2005) Interaction network among *Escherichia coli*
700 membrane proteins involved in cell division as revealed by bacterial two-hybrid analysis. *J*
701 *Bacteriol* **187**: 2233-2243.
702 Karimova, G., Pidoux, J., Ullmann, A. and Ladant, D. (1998) A bacterial two-hybrid system
703 based on a reconstituted signal transduction pathway. *Proc Natl Acad Sci USA* **95**: 5752-
704 5756.
705 Karimova, G., Robichon, C. and Ladant, D. (2009) Characterization of YmgF, a 72-residue
706 inner membrane protein that associates with the *Escherichia coli* cell division machinery.
707 *J Bacteriol* **191**: 333-346.
708 Karimova, G., Ullmann, A. and Ladant, D. (2001) Protein-protein interaction between
709 *Bacillus stearothermophilus* tyrosyl-tRNA synthetase subdomains revealed by a bacterial
710 two-hybrid system. *J Mol Microbiol Biotechnol* **3**: 73-82.

711 Karuppiah, V. and Derrick, J.P. (2011) Structure of the PilM-PilN inner membrane type IV
712 pilus biogenesis complex from *Thermus thermophilus*. *J Biol Chem* **27**: 24434-24442.
713 Krogh, A., Larsson, B., von Heijne, G. and Sonnhammer, E.L. (2001) Predicting
714 transmembrane protein topology with a hidden Markov model: application to complete
715 genomes. *J Mol Biol* **305**: 567-580.
716 Maier, B., Potter, L., So, M., Long, C.D., Seifert, H.S. and Sheetz, M.P. (2002) Single pilus
717 motor forces exceed 100 pN. *Proc Natl Acad Sci USA* **99**: 16012-16017.
718 Mattick, J.S. (2002) Type IV pili and twitching motility. *Annu Rev Microbiol* **56**: 289-314.
719 Mehr, I.J., Long, C.D., Serkin, C.D. and Seifert, H.S. (2000) A homologue of the
720 recombination-dependent growth gene, *rdgC*, is involved in gonococcal pilin antigenic
721 variation. *Genetics* **154**: 523-532.
722 Merz, A.J., So, M. and Sheetz, M.P. (2000) Pilus retraction powers bacterial twitching
723 motility. *Nature* **407**: 98-102.
724 Parge, H.E., Forest, K.T., Hickey, M.J., Christensen, D.A., Getzoff, E.D. and Tainer, J.A.
725 (1995) Structure of the fibre-forming protein pilin at 2.6 Å resolution. *Nature* **378**: 32-38.
726 Pelicic, V. (2008) Type IV pili: *e pluribus unum*? *Mol Microbiol* **68**: 827-837.
727 Pujol, C., Eugène, E., de Saint Martin, L. and Nassif, X. (1997) Interaction of *Neisseria*
728 *meningitidis* with a polarized monolayer of epithelial cells. *Infect Immun* **65**: 4836-4842.
729 Ramer, S.W., Schoolnik, G.K., Wu, C., Hwang, J., Schmidt, S.A. and Bieber, D. (2002) The
730 type IV pilus assembly complex: biogenic interaction among the bundle-forming pilus
731 proteins of enteropathogenic *Escherichia coli*. *J Bacteriol* **184**: 3457-3465.
732 Rusniok, C.*, et al.* (2009) NeMeSys: a resource for narrowing the gap between sequence
733 and function in the human pathogen *Neisseria meningitidis*. *Genome Biol* **10**: R110.
734 Sambrook, J. and Russell, D.W. (2001) *Molecular cloning. A laboratory manual*. Cold Spring
735 Harbor Laboratory Press, Cold Spring Harbor, New York.

736 Sampaleanu, L.M.*, et al.* (2009) Periplasmic domains of *Pseudomonas aeruginosa* PilN and
737 PilO form a stable heterodimeric complex. *J Mol Biol* **394**: 143-159.
738 Satyshur, K.A., Worzalla, G.A., Meyer, L.S., Heiniger, E.K., Aukema, K.G., Misic, A.M. and
739 Forest, K.T. (2007) Crystal structures of the pilus retraction motor PilT suggest large
740 domain movements and subunit cooperation drive motility. *Structure* **15**: 363-376.
741 Sauer, F.G., Mulvey, M.A., Schilling, J.D., Martinez, J.J. and Hultgren, S.J. (2000) Bacterial
742 pili: molecular mechanisms of pathogenesis. *Curr Opin Microbiol* **3**: 65-72.
743 Savvides, S.N. (2007) Secretion superfamily ATPases swing big. *Structure* **15**: 255-257.
744 Strom, M.S., Nunn, D.N. and Lory, S. (1993) A single bifunctional enzyme, PilD, catalyzes
745 cleavage and N-methylation of proteins belonging to the type IV pilin family. *Proc Natl*
746 *Acad Sci USA* **90**: 2404-2408.
747 Tammam, S.*, et al.* (2011) Characterization of the PilN, PilO and PilP type IVa pilus
748 subcomplex. *Mol Microbiol* **82**: 1496-1514.
749 Uetz, P. and Hughes, R.E. (2000) Systematic and large-scale two-hybrid screens. *Curr Opin*
750 *Microbiol* **3**: 303-308.
751 Wolfgang, M., Park, H.S., Hayes, S.F., van Putten, J.P. and Koomey, M. (1998) Suppression
752 of an absolute defect in type IV pilus biogenesis by loss-of-function mutations in *pilT*, a
753 twitching motility gene in *Neisseria gonorrhoeae*. *Proc Natl Acad Sci USA* **95**: 14973-
754 14978.
755 Wolfgang, M., van Putten, J.P., Hayes, S.F., Dorward, D. and Koomey, M. (2000)
756 Components and dynamics of fiber formation define a ubiquitous biogenesis pathway for
757 bacterial pili. *EMBO J* **19**: 6408-6418.
758

FIGURES

Figure 1.

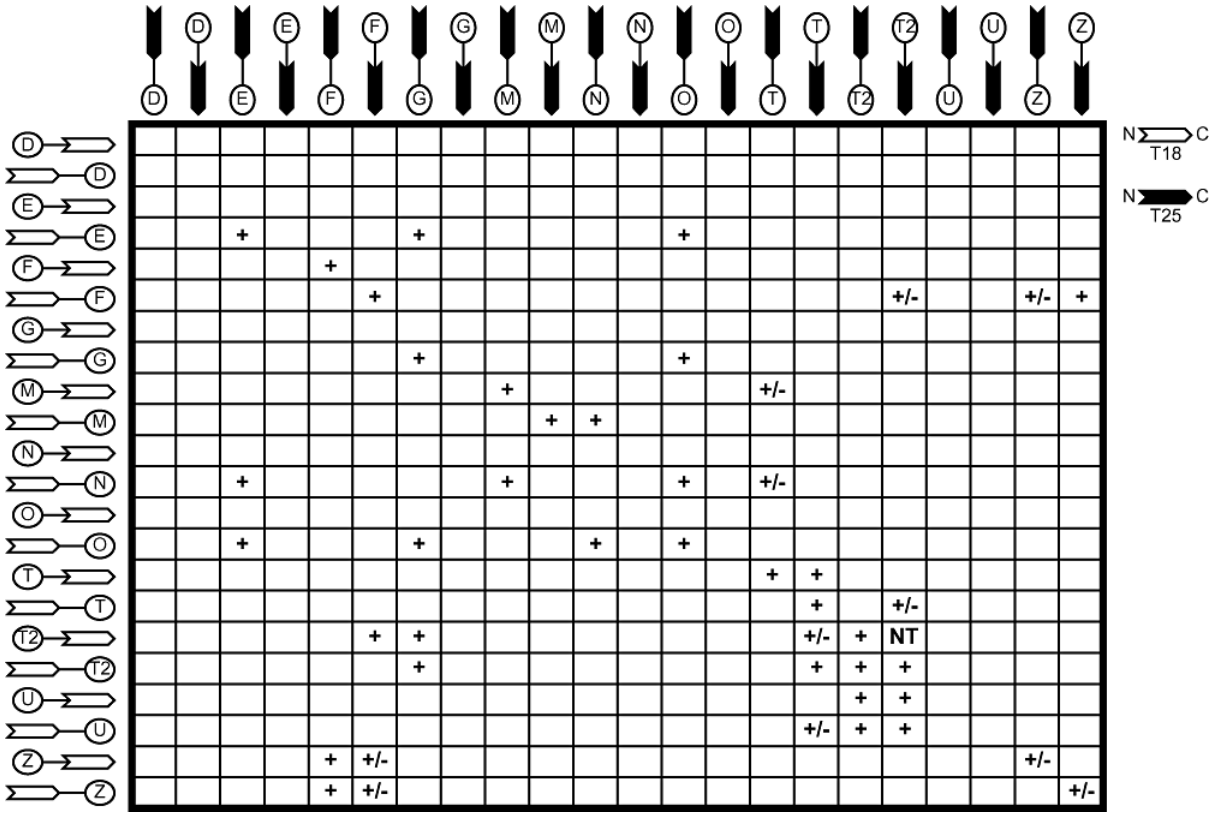

Binary interactions between *N. meningitidis* Pil proteins identified using a bacterial adenylate cyclase two hybrid (BACTH). Eleven Pil proteins, indicated by their corresponding letter (*e.g.* D stands for PilD), were fused to both the N- or C-termini of the *B. pertussis* adenylate cyclase fragments T18 or T25, respectively. All the possible T18+T25 plasmid combinations, 484 in total, were co-transformed in the *E. coli cya* strain BTH101 and plated on MacConkey agar plates supplemented with maltose. Functional complementation between the T18 and T25 fragments, which occurs only upon interaction of the hybrid proteins, triggers the expression of *mal* genes and yields pink to purple colonies (Karimova *et al.*, 1998). +, pairs that yielded coloured colonies. +/-, only a fraction of the colonies were pink. NT, this combination could not be tested because the colonies were microscopic even after prolonged incubation.

Figure 2.

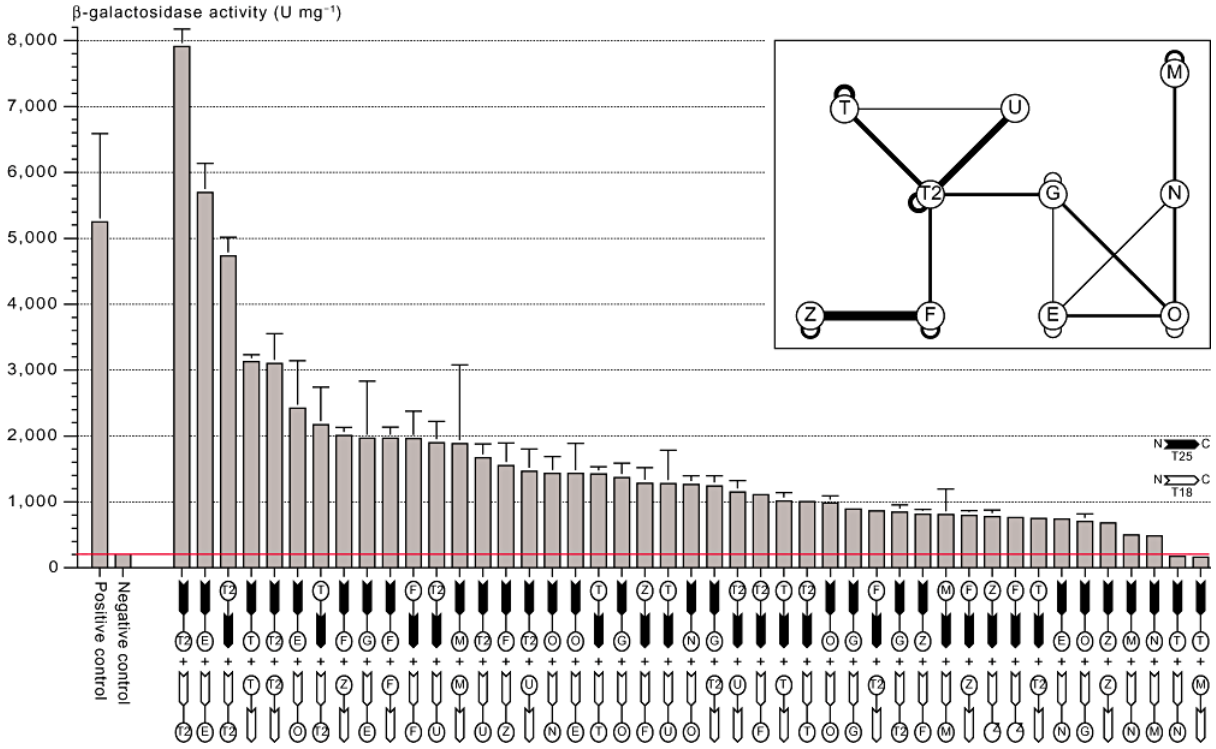

Quantification of Pil-Pil interaction identified by BACTH. The efficiency of functional complementation between the indicated hybrid proteins was quantified by measuring ß-galactosidase activities. As a positive control, we used a strain co-transformed with pUT18C-zip and pKT25-zip, in which the T18-Zip and T25-Zip hybrid proteins interact through a leucine zipper motif (Karimova *et al.*, 1998). As a negative control, we used a strain co-transformed with pUT18C and pKT25 plasmids containing no inserts. Results are expressed as units of β-galactosidase activity/mg of bacteria (dry weight) and are the mean ± standard deviation of at least three independent experiments. The red line indicates the background β-galactosidase activity measured in the negative control. The inset is a graphical representation of the protein network that was identified. The thickness of the edges between nodes is proportional to the number of times that link has been identified (between one and six times).

Figure 3.

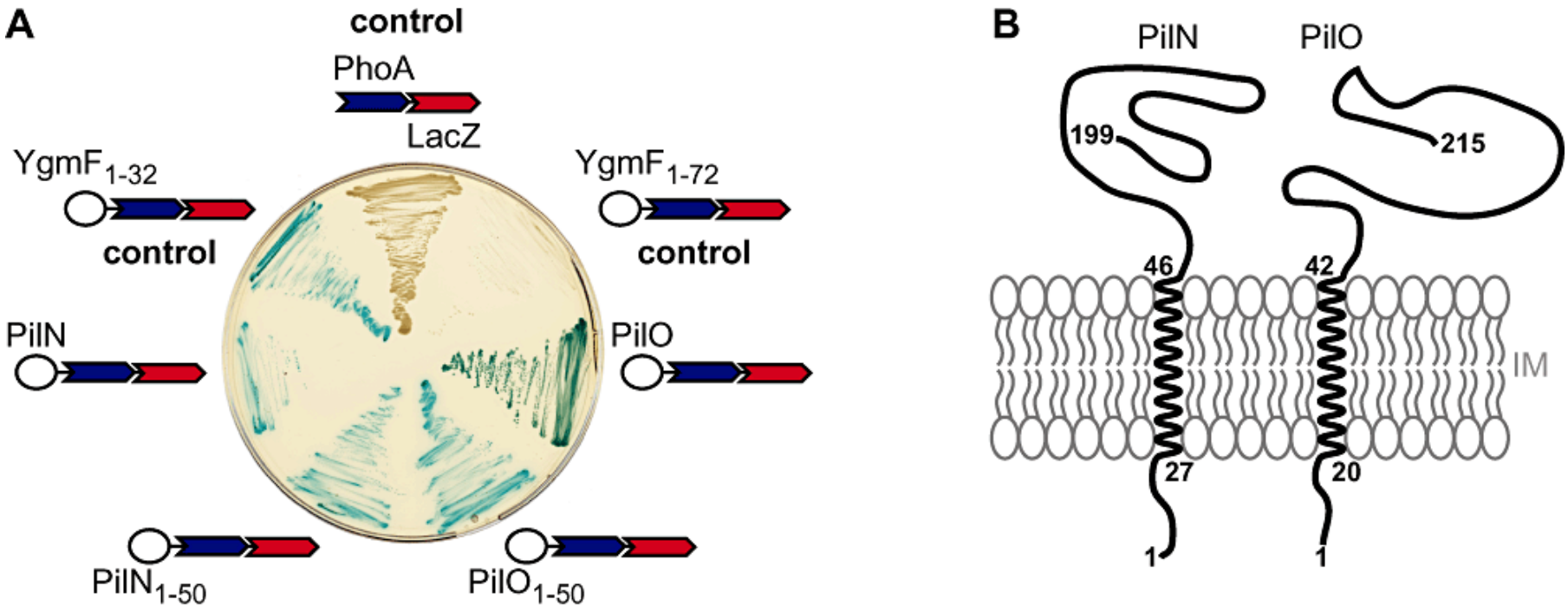

Membrane topology of PilN and PilO. (**A**) *pilN* and *pilO* genes encoding full-length or truncated proteins (*i.e*. the first 50 residues) were fused in frame to a dual *pho-lac* reporter in the pKTop vector (Karimova *et al.*, 2009). *E. coli* DH5α transformants expressing the different Pho-Lac fusions were plated on LB medium containing the chromogenic substrate of alkaline phosphatase, X-Phos. As controls directing the reporter either to the periplasm ($YmgF_{1-32}$-PhoLac) or the cytoplasm ($YmgF_{1-72}$-PhoLac) we used two previously published fusions with the polytopic protein YmgF from *E.coli* (Karimova *et al.*, 2009). *E. coli* DH5 (pKTop) was also included as a control. Blue coloration of the colonies (high phosphatase activity) indicates that the phosphatase is on the periplasmic side of the inner membrane. No coloration of the colonies indicates that the phosphatase is on the cytoplasmic side of the inner membrane. (**B**) Schematic representation of the topology of PilN and PilO. The transmembrane helices have been predicted using TMHMM (Krogh *et al.*, 2001). IM, inner membrane.

Figure 4.

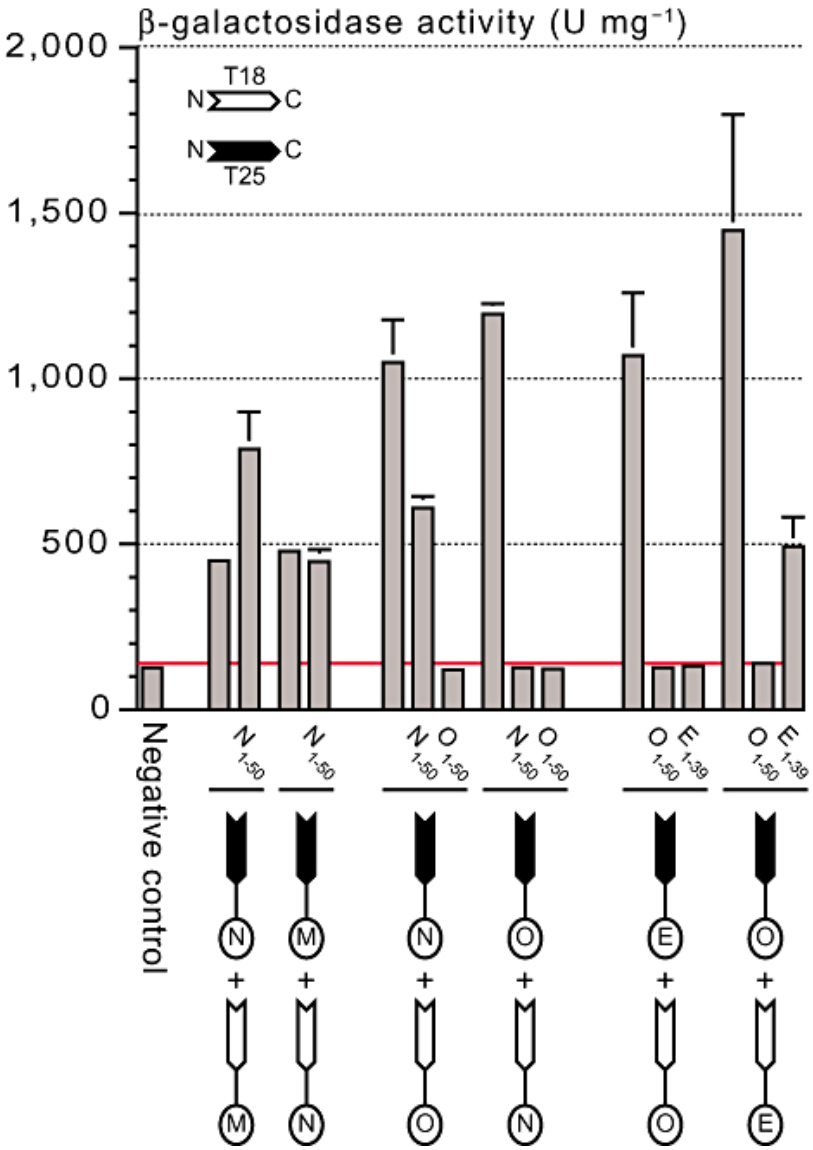

Mapping interacting domains between PilE, PilM, PilN and PilO by BACTH. Truncated variants of PilE, PilN and PilO fused to T18 and/or T25 fragments were constructed. The strength of each interaction was quantified by measuring ß-galactosidase activities and compared to the strength of the interaction with the full-length protein (where not indicated, both proteins are full-length). Results are expressed as units of β-galactosidase activity/mg of bacteria (dry weight) and are the mean ± standard deviation of at least three independent experiments. The red line indicates the background β-galactosidase activity measured in the negative control.

Figure 5.

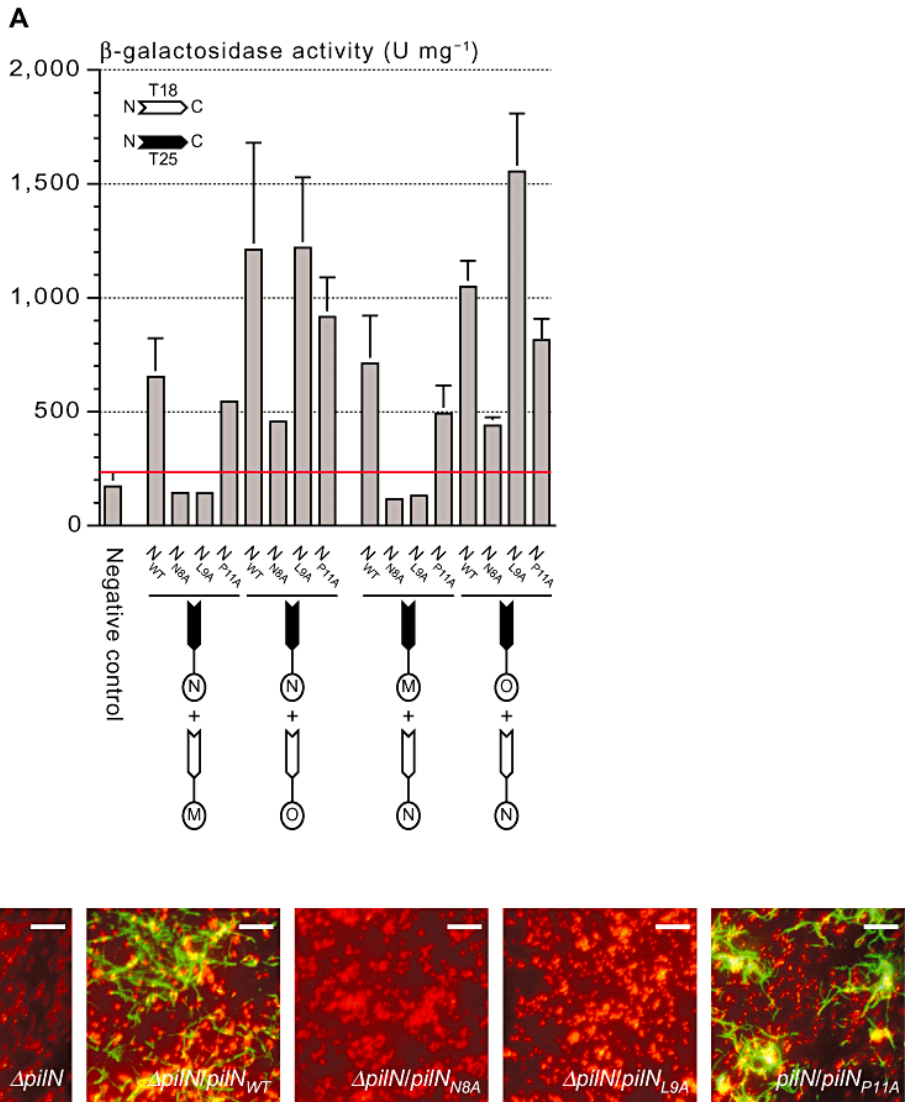

Functional importance of the widely conserved N-terminal INLLPY motif in the cytosolic segment of PilN. (**A**) Mutant *pilN* alleles which encode $PilN_{N8A}$, $PilN_{L9A}$ and $PilN_{P11A}$ variants, were fused to the C-terminus of the T18 and T25 fragments. The efficiency of functional complementation between these hybrid proteins (and $PilN_{WT}$ used as a positive control) and PilM or PilO fused to the C-terminus of the T18 and T25 fragments was quantified by measuring ß-galactosidase activities and compared to the strength of the interaction with the WT protein. Results are expressed as units of β-galactosidase activity/mg of bacteria (dry

820 weight) and are the mean ± standard deviation of at least three independent experiments.
821 The red line indicates the background β-galactosidase activity measured in the negative
822 control. (**B**) Piliation as assessed by immunofluorescence microscopy in *N. meningitidis*
823 *ΔpilN/pilN*$_{N8A}$, *ΔpilN/pilN*$_{L9A}$ and *ΔpilN/pilN*$_{P11A}$ strains in which the corresponding *pilN* alleles
824 generated by site-directed mutagenesis and placed under the control of an IPTG-inducible
825 promoter were integrated ectopically into the genome of a *ΔpilN* non polar mutant. The WT
826 strain, *ΔpilN* mutant and *ΔpilN/pilN*$_{WT}$ complemented mutant were included as controls. Tfp
827 (green filaments) were labelled with a monoclonal antibody specific for *N. meningitidis* 8013
828 filaments (Pujol *et al.*, 1997), while the bacteria (red) were stained with DAPI. Scale bar
829 represent 10 µm.
830
831

832

Figure 6.

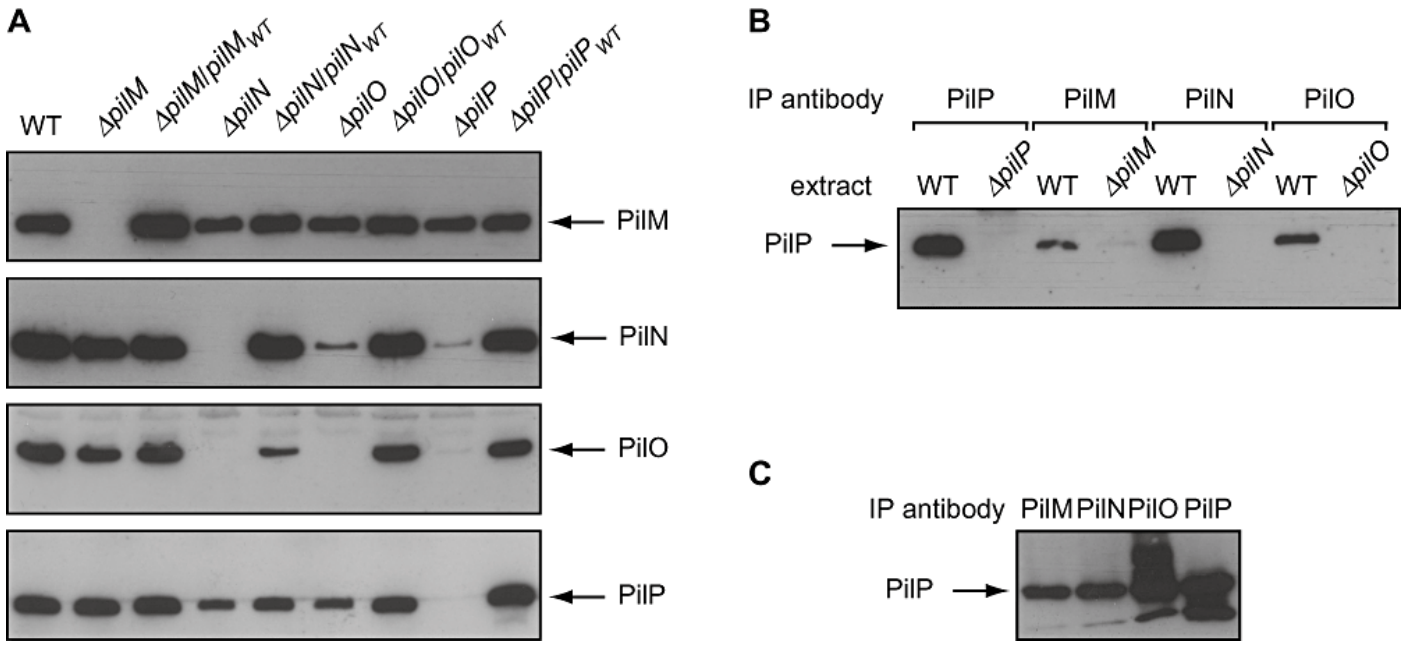

Identification of interactions between PilP and PilM, PilN and PilO by determining stability of each protein by immunoblotting in non polar *ΔpilM*, *ΔpilN*, *ΔpilO* and *ΔpilP* mutants and/or by performing co-immunoprecipitations. (**A**) PilM, PilN, PilO an PilP were detected by immunoblotting in whole-cell protein extracts of non polar *ΔpilM*, *ΔpilN*, *ΔpilO* and *ΔpilP* mutants and *ΔpilM/pilM*$_{WT}$, *ΔpilN/pilN*$_{WT}$, *ΔpilO/pilO*$_{WT}$ and *ΔpilP/pilP*$_{WT}$ complemented strains. The WT strain was included as a positive control. For each blot, equal amounts of whole cell extracts were loaded in each lane. (**B**) Identical amounts of B-PER protein extracts (500 µg) from *N. meningitidis* WT strain or *ΔpilM*, *ΔpilN*, *ΔpilO* and *ΔpilP* non polar mutants (as controls) were immunoprecipitated using anti-PilM, anti-PilN, anti-PilO and anti-PilP antibodies. Ten µl of precipitates were subsequently probed for the presence of PilP by immunoblotting using an anti-PilP serum. It should be noted that since the signal was much stronger in the precipitates of the WT strain obtained using anti-PilP and anti-PilN antibodies, these have been diluted prior SDS-PAGE 100- and 50-fold, respectively. (**C**) B-PER protein extracts from an *E. coli* BL21 (pACYCDuet pil*MNOP*) strain engineered to co-express PilM, PilN, PilO and PilP were immunoprecipitated using anti-PilM, anti-PilN, anti-PilO and anti-PilP antibodies. Ten µl of precipitates were subsequently probed for the presence of PilP by immunoblotting.

Figure 7.

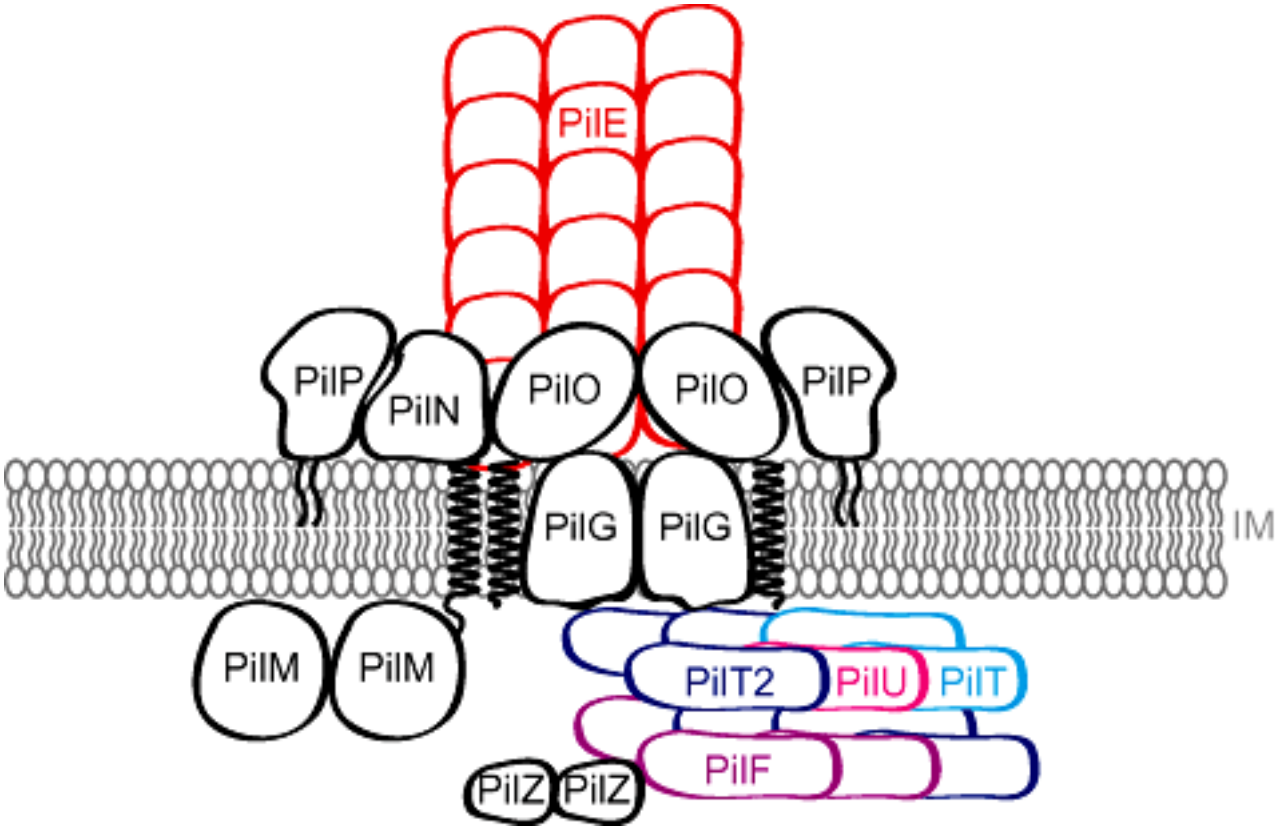

Schematic representation of the interactions between the proteins of the Tfp machinery as determined in this study. For the sake of clarity, the proteins in this cartoon are not drawn to scale.

851 **Table 1**. Primers used in this study.

Name	Sequence*	Used for
dir PilD	cccggatccATGTCTGATTTGTCTGTATTGTCGC	cloning *pilD* in BACTH vectors
rev PilD	cgcggtaccgCAGCACCGGATGGGTCAGCCACC	cloning *pilD* in BACTH vectors
rev PilE	cgcggtaccgGCTGGCAGATGAATCATCGC	cloning *pilE* in BACTH vectors
dir PilE	cgcggatccATGAACACCCTTCAAAAAGGTT	cloning *pilE* in BACTH vectors
rev $PilE_{1-39}$	cgcggtaccgTTGTGCGCGGGCTGTGTAGT	cloning truncated *pilE* in BACTH vectors
dir PilF	cgcggatccATGAGCGTAGGTTTGCTGAGG	cloning *pilF* in BACTH vectors
rev PilF	cgcggtaccgATCGTTGGTATTTGCCGTTAC	cloning *pilF* in BACTH vectors
dir PilG	cgcggatccATGGCTAAAAACGGAGGATTTTCTTTGTTCGC	cloning *pilG* in BACTH vectors
rev PilG	cgcggtaccgGGCGACCACGTTGCCCAAA	cloning *pilG* in BACTH vectors
dir PilM	cgcggatccATGCGCTTGTTTAAAAGCTTG	cloning *pilM* in BACTH vectors
rev PilM	cgcggtaccgTAATCCCCGTACCGCCA	cloning *pilM* in BACTH vectors
dir PilN	cccggatccATGAACAATTTAATCAAAATCAACC	cloning *pilN* in BACTH vectors
rev PilN-bis	cgcggtaccgGTTTGCCTCCTGTGCGTTTCCC	cloning *pilN* in BACTH vectors
rev $PilN_{1-50}$	cgcggtaccgGATCATATTGTCGATAAACAGG	cloning truncated *pilN* in BACTH and pKTop vectors
dir PilO	cccggatccATGGCTTCTAAATCATCTAAAAC	cloning *pilO* in BACTH vectors
rev PilO-bis	cgcggtaccgTTTTTGCTCGGCATTTTGTGCC	cloning *pilO* in BACTH vectors
rev $PilO_{1-50}$	cgcggtaccgAAGGGATTCCATCTGGCTTTTG	cloning truncated *pilO* in BACTH and pKTop vectors
dir PilT	cgcggatccATGCAGATTACCGACTTACTCGC	cloning *pilT* in BACTH vectors
rev pilT	cgcggtaccgGAAACTCATACTTTCGCTGTT	cloning *pilT* in BACTH vectors
dir PilT2	cgcggatccATGACCGCAAAGGAAGAACTG	cloning *pilT2* in BACTH vectors
rev PilT2	cgcggtaccgGAGCAGTTCCAAATCGGGGC	cloning *pilT2* in BACTH vectors
dir PilU	cgcggatccATGAATACCGATAACCTGCACG	cloning *pilU* in BACTH vectors
rev PilU	cgcggtaccgGGAAATGAGGTTGAGACCG	cloning *pilU* in BACTH vectors
dir Nm981	cgcggatccATGTCAGACGGACAAAATATTCC	cloning *pilZ* in BACTH vectors
rev Nm981	cgcggtaccgCATGGTAAACGTAGGTCTG	cloning *pilZ* in BACTH vectors
*pilM*f	catATGCGCTTGTTTAAAAGC	cloning *pilM* in pET-14b
*pilM*r	ggatccTTATAATCCCCGTACCGCC	cloning *pilM* in pET-14b
pilM-2x-F	cgcgaattcATGCGCTTGTTTAAAAGCTTG	cloning *pilM* in pMal-c2X

pilM-2x-R	cgcgtcgacTTATAATCCCCGTACCGCCA	cloning *pilM* in pMal-c2X
pilN-2X-F	cgcgaattcGACAATATGATCAATAACCAGT	cloning *pilN* in pMal-c2X
pilN-2x-R	cgcctgcagTCAGTTTGCCTCCTGTGCGT	cloning *pilN* in pMal-c2X
pilO-2x-F	cgcgaattcTTCAAAAGCCAGATGGAATCC	cloning *pilO* in pMal-c2X
pilO-2x-R	cgcctgcagTTATTTTTGCTCGGCATTTTGTG	cloning *pilO* in pMal-c2X
pilP F-Eco	ggatatcCGCGAAGCCAAAGCAGAAATCATAC	cloning *pilP* in pET-20b
pilP R-Xho	ccgctcgaGTTCTGCTTTACGGGAAACCCAGTT	cloning *pilP* in pET-20b
*pilMNOP*DuetF	ggcatATGCGCTTGTTTAAAAGCTTGA	cloning *pilMNOP* in Duet co-expression vector
*pilMNOP*DuetR	ggctcgagTTAATTTTGTTCTGCGGCAGG	cloning *pilMNOP* in Duet co-expression vector
aphF	ATGGCTAAAATGAGAATATCACC	creation of non-polar *ΔpilM*, *ΔpilN*, *ΔpilO*, and *ΔPilP* mutants
aphR	CTAAAACAATTCATCCAGTAAAA	creation of non-polar *ΔpilM*, *ΔpilN*, *ΔpilO*, and *ΔPilP* mutants
pilM-F1	CTGCTGCGTAATCGTACTCG	creation of non-polar *ΔpilM* mutant
pilM-R1	ggtgatattctcattttagccatGATGAAAGTTCCTGCTTTATTTGTA	creation of non-polar *ΔpilM* mutant
pilM-F2	ttttactggatgaattgttttagGTTCGGTTTGGCGGTACGGGGATTAT	creation of non-polar *ΔpilM* mutant
pilM-R2	ttcagacggcatAGCCGGATTCTCTTTGGATT	creation of non-polar *ΔpilM* mutant
pilN-F1	atgccgtctgaaGAAATCGAACCCCTGATTGA	creation of non-polar *ΔpilN* mutant
pilN-R1	ggtgatattctcattttagccatAATTATAATCCCCGTACCGC	creation of non-polar *ΔpilN* mutant
pilN-F2	ttttactggatgaattgttttagGCTTCGGGAAACGCACAGGA	creation of non-polar *ΔpilN* mutant
pilN-R2	ttcagacggcatGAGGTTCAGGATGCTGCTCT	creation of non-polar *ΔpilN* mutant
pilO-F1	TCCCCTACAGGGAAGAGATG	creation of non-polar *ΔpilO* mutant
pilO-R1	ggtgatattctcattttagccatTCAGTTTGCCTCCTGTGCGTTTCC	creation of non-polar *ΔpilO* mutant
pilO-F2	ttttactggatgaattgttttagCGAGCAAAAATAActtacgttaggg	creation of non-polar *ΔpilO* mutant
pilO-R2	ttcagacggcatGCTTTACGGGAAACCCAGTT	creation of non-polar *ΔpilO* mutant
pilP-F1	CAACAACCTTCACCTGCTCA	creation of non-polar *ΔpilP* mutant
pilP-R1	ggtgatattctcattttagccatGGTTTCCCTAACGTAAGTTATTTTTGC	creation of non-polar *ΔpilP* mutant
pilP-F2	ttttactggatgaattgttttagCGCAGAACAAAATTAAgaagaggattact	creation of non-polar *ΔpilP* mutant
pilP-R2	ttcagacggcatTACGGATACTGCGGACTTGG	creation of non-polar *ΔpilP* mutant
dir $PilN_{N8A}$	GAACAATTTAATCAAAATC**GC**CCTCCTCCCCTACAGGGAAG	site-directed mutagenesis of *pilN*

rev PilN$_{N8A}$	CTTCCCTGTAGGGGAGGAGG**GC**GATTTTGATTAAATTGTTC	site-directed mutagenesis of *pilN*
dir PilN$_{L9A}$	CAATTTAATCAAAATCAAC**GC**CCTCCCCTACAGGGAAGAG	site-directed mutagenesis of *pilN*
rev PilN$_{L9A}$	CTCTTCCCTGTAGGGGAGG**GC**GTTGATTTTGATTAAATTG	site-directed mutagenesis of *pilN*
dir PilN$_{P11A}$	CAAAATCAACCTCCTC**G**CCTACAGGGAAGAGATG	site-directed mutagenesis of *pilN*
rev PilN$_{P11A}$	CATCTCTTCCCTGTAGG**C**GAGGAGGTTGATTTTG	site-directed mutagenesis of *pilN*
pilN-IndF	cc<u>ttaattaa</u>ggagtaattttATGAACAATTTAATCAAAATCAAC	cloning *pilN* in pGCC4
pilN-IndR	cc<u>ttaattaa</u>TCAGTTTGCCTCCTGTGCGTT	cloning *pilN* in pGCC4

852 * Lower-case is used for overhangs. Restriction sites are underlined. Mismatched bases generating mutations are in bold.

853 **Table 2.** Plasmids used in this study.

Name	Description/Purpose	Source/Reference
pCRII-TOPO	TA cloning vector for direct ligation of PCR products	Invitrogen
pYU9	*pilM* flanked by *Nde*I + *Bam*HI in pCRII-TOPO	this study
TOPO *pilP*	*pilP* fragment flanked by *Eco*RI + *Xho*I in pCRII-TOPO	this study
PCR8/GW/TOPO	TA cloning vector for direct ligation of PCR products	Invitrogen
pYU60	*pilE* flanked by *Bam*HI + *Kpn*I in PCR8/GW/TOPO	this study
pYU61	*pilN* flanked by *Bam*HI + *Kpn*I in PCR8/GW/TOPO	this study
pYU62	*pilO* flanked by *Bam*HI + *Kpn*I in PCR8/GW/TOPO	this study
pYU70	*pilT2* flanked by *Bam*HI + *Kpn*I in PCR8/GW/TOPO	this study
pYU71	*pilZ* flanked by *Bam*HI + *Kpn*I in PCR8/GW/TOPO	this study
pYU72	*pilD* flanked by *Bam*HI + *Kpn*I in PCR8/GW/TOPO	this study
pYU73	*pilF* flanked by *Bam*HI + *Kpn*I in PCR8/GW/TOPO	this study
pYU74	*pilG* flanked by *Bam*HI + *Kpn*I in PCR8/GW/TOPO	this study
pYU75	*pilM* flanked by *Bam*HI + *Kpn*I in PCR8/GW/TOPO	this study
pYU76	*pilT* flanked by *Bam*HI + *Kpn*I in PCR8/GW/TOPO	this study
pYU77	*pilU* flanked by *Bam*HI + *Kpn*I in PCR8/GW/TOPO	this study
TOPO $pilE_{short}$	truncated *pilE* flanked by *Bam*HI + *Kpn*I in PCR8/GW/TOPO	this study
TOPO $pilN_{short}$	truncated *pilN* flanked by *Bam*HI + *Kpn*I in PCR8/GW/TOPO	this study
TOPO $pilO_{short}$	truncated *pilO* flanked by *Bam*HI + *Kpn*I in PCR8/GW/TOPO	this study
TOPO $pilE_{N8A}$	mutant *pilN* allele flanked by *Bam*HI + *Kpn*I in PCR8/GW/TOPO	this study
TOPO $pilE_{L9A}$	mutant *pilN* allele flanked by *Bam*HI + *Kpn*I in PCR8/GW/TOPO	this study
TOPO $pilE_{P11A}$	mutant *pilN* allele flanked by *Bam*HI + *Kpn*I in PCR8/GW/TOPO	this study
pUT18	BACTH vector designed to express a protein fused in frame at its C-terminus with T18; ColE1 ori; Amp^R	(Karimova *et al.*, 2001)
pUT18 *pilD*	BACTH vector expressing PilD-T18	this study
pUT18 *pilE*	BACTH vector expressing PilE-T18	this study
pUT18 *pilF*	BACTH vector expressing PilF-T18	this study
pUT18 *pilG*	BACTH vector expressing PilG-T18	this study
pUT18 *pilM*	BACTH vector expressing PilM-T18	this study
pUT18 *pilN*	BACTH vector expressing PilN-T18	this study

pUT18 *pilO*	BACTH vector expressing PilO-T18	this study
pUT18 *pilT*	BACTH vector expressing PilT-T18	this study
pUT18 *pilT2*	BACTH vector expressing PilT2-T18	this study
pUT18 *pilU*	BACTH vector expressing PilU-T18	this study
pUT18 *pilZ*	BACTH vector expressing PilZ-T18	this study
pUT18C	BACTH vector designed to express a protein fused in frame at its N-terminus with T18; ColE1 ori; Amp^R	(Karimova *et al.*, 2001)
pUT18C *pilD*	BACTH vector expressing T18-PilD	this study
pUT18C *pilE*	BACTH vector expressing T18-PilE	this study
pUT18C $pilE_{short}$	BACTH vector expressing T18-$PilE_{1-39}$	this study
pUT18C *pilF*	BACTH vector expressing T18-PilF	this study
pUT18C *pilG*	BACTH vector expressing T18-PilG	this study
pUT18C *pilM*	BACTH vector expressing T18-PilM	this study
pUT18C *pilN*	BACTH vector expressing T18-PilN	this study
pUT18C $pilN_{short}$	BACTH vector expressing T18-$PilN_{1-50}$	this study
pUT18C $pilN_{N8A}$	BACTH vector expressing T18-$PilN_{N8A}$	this study
pUT18C $pilN_{L9A}$	BACTH vector expressing T18-$PilN_{L9A}$	this study
pUT18C $pilN_{P11A}$	BACTH vector expressing T18-$PilN_{P11A}$	this study
pUT18C *pilO*	BACTH vector expressing T18-PilO	this study
pUT18C $pilO_{short}$	BACTH vector expressing T18-$PilO_{1-50}$	this study
pUT18C *pilT*	BACTH vector expressing T18-PilT	this study
pUT18C *pilT2*	BACTH vector expressing T18-PilT2	this study
pUT18C *pilU*	BACTH vector expressing T18-PilU	this study
pUT18C *pilZ*	BACTH vector expressing T18-PilZ	this study
pKT25	BACTH vector designed to express a protein fused in frame at its N-terminus with T25; p15 ori; Km^R	(Karimova *et al.*, 2001)
pKT25 *pilD*	BACTH vector expressing T25-PilD	this study
pKT25 *pilE*	BACTH vector expressing T25-PilE	this study
pKT25 $pilE_{short}$	BACTH vector expressing T25-$PilE_{1-39}$	this study
pKT25 *pilF*	BACTH vector expressing T25-PilF	this study
pKT25 *pilG*	BACTH vector expressing T25-PilG	this study
pKT25 *pilM*	BACTH vector expressing T25-PilM	this study
pKT25 *pilN*	BACTH vector expressing T25-PilN	this study

pKT25 *pilN*$_{short}$	BACTH vector expressing T25-PilN$_{1-50}$	this study
pKT25 *pilN*$_{N8A}$	BACTH vector expressing T25-PilN$_{N8A}$	this study
pKT25 *pilN*$_{L9A}$	BACTH vector expressing T25-PilN$_{L9A}$	this study
pKT25 *pilN*$_{P11A}$	BACTH vector expressing T25-PilN$_{P11A}$	this study
pKT25 *pilO*	BACTH vector expressing T25-PilO	this study
pKT25 *pilO*$_{short}$	BACTH vector expressing T25-PilO$_{1-50}$	this study
pKT25 *pilT*	BACTH vector expressing T25-PilT	this study
pKT25 *pilT2*	BACTH vector expressing T25-PilT2	this study
pKT25 *pilU*	BACTH vector expressing T25-PilU	this study
pKT25 *pilZ*	BACTH vector expressing T25-PilZ	this study
pKNT25	BACTH vector designed to express a protein fused in frame at its C-terminus with T25; p15 ori; Km^R	(Karimova *et al.*, 2001)
pKNT25 *pilD*	BACTH vector expressing PilD-T25	this study
pKNT25 *pilE*	BACTH vector expressing PilE-T25	this study
pKNT25 *pilF*	BACTH vector expressing PilF-T25	this study
pKNT25 *pilG*	BACTH vector expressing PilG-T25	this study
pKNT25 *pilM*	BACTH vector expressing PilM-T25	this study
pKNT25 *pilN*	BACTH vector expressing PilN-T25	this study
pKNT25 *pilO*	BACTH vector expressing PilO-T25	this study
pKNT25 *pilT*	BACTH vector expressing PilT-T25	this study
pKNT25 *pilT2*	BACTH vector expressing PilT2-T25	this study
pKNT25 *pilU*	BACTH vector expressing PilU-T25	this study
pKNT25 *pilZ*	BACTH vector expressing PilZ-T25	this study
pKTop	vector designed to determine the topology of a protein by fusing it at its C-terminus with the dual reporter PhoA$_{22-472}$/LacZ$_{4-60}$	(Karimova *et al.*, 2009)
pKTop YmgF$_{1-32}$	pKTop expressing YmgF$_{1-32}$-PhoA-LacZ	(Karimova *et al.*, 2009)
pKTop YmgF$_{1-72}$	pKTop expressing YmgF$_{1-72}$-PhoA-LacZ	(Karimova *et al.*, 2009)
pKTop *pilN*	pKTop expressing PilN-PhoA-LacZ	this study
pKTop *pilN*$_{short}$	pKTop expressing PilN$_{1-50}$-PhoA-LacZ	this study
pKTop *pilO*	pKTop expressing PilN-PhoA-LacZ	this study
pKTop *pilO*$_{short}$	pKTop expressing PilN$_{1-50}$-PhoA-LacZ	this study
pGCC4	integrative vector for expressing *Neisseria* genes under the transcriptional	(Mehr *et al.*, 2000)

	control of an IPTG-inducible promoter	
pYU26	*pilN* in pGCC4	(Carbonnelle *et al.*, 2006)
pGCC4 *pilN*$_{N8A}$	*pilN*$_{N8A}$ in pGCC4	this study
pGCC4 *pilN*$_{L9A}$	*pilN*$_{L9A}$ in pGCC4	this study
pGCC4 *pilN*$_{P11A}$	*pilN*$_{P11A}$ in pGCC4	this study
pYU25	*pilM* in pGCC4	(Carbonnelle *et al.*, 2006)
pYU27	*pilO* in pGCC4	(Carbonnelle *et al.*, 2006)
pYU28	*pilP* in pGCC4	(Carbonnelle *et al.*, 2006)
pET-14b	expression vector; the given protein is fused at its N-terminus with a His-Tag	Novagen
pYU12	pET-14b derivative for expressing full-length PilM	this study
pET-20b	expression vector; the protein is fused at its C-terminus with a His-Tag	Novagen
pET20-*pilP*	pET-20b derivative for expressing residues 17-145 of mature PilP	this study
pACYCDuet-1	co-expression vector	Novagen
pACYCDuet pil*MNOP*	pACYCDuet-1 derivative for co-expressing PilM, PilN, PilO and PilP	this study
pMal-c2x	expression vector; the protein is fused at its N-terminus with maltose-binding protein (MBP) and directed to the cytoplasm	New England Biolabs
pYU42	pMal-c2x derivative for expressing MBP-PilM	this study
pYU44	pMal-c2x derivative for expressing MBP-PilO	this study
pYU51	pMal-c2x derivative for expressing MBP-PilN	this study

854